

**Development of an Infrared Gaseous Radiation Band Model
Based on NASA SP-3080 for Computational Fluid
Dynamic Code Validation Applications**

by

Edward L. Nelson

Thesis Submitted to the Faculty of the
Virginia Polytechnic Institute and State University
in partial fulfillment of the requirements of the degree of
Master of Science in Mechanical Engineering

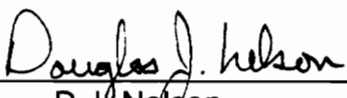
APPROVED:



J.R. Mahan, Chairman



C.H. Stern



D.J. Nelson

August 1992
Blacksburg, VA

C.2

LD
5655
V855
1992
N457
C.2

**Development of an Infrared Gaseous Radiation Band Model
Based on NASA SP-3080 for Computational Fluid
Dynamic Code Validation Applications**

by

Edward L. Nelson

Dr. J.R. Mahan, Chairman

(ABSTRACT)

The increased use of infrared imaging as a flow visualization technique and as a validation technique for computational fluid dynamics (CFD) codes has led to an in-depth study of infrared band models. The ability to create fast and accurate images of airframe and plume infrared emissions often depends on the complexity of the band model. An infrared band model code has been created based largely on the band model published in NASA SP-3080, **Handbook of Infrared Radiation from Combustion Gases**. Improvements to the NASA SP-3080 model using the NIRATAM data files have been made. The model and its theoretical basis are thoroughly described. Results are presented and are compared with results from the band models contained in SCORPIO and LOIR.

Acknowledgements

The work presented in this thesis is the product of unselfish work from many people on both coasts of the United States. Virginia Polytechnic Institute and State University (VPI&SU) in Blacksburg, VA, and the National Aeronautics and Space Administration (NASA) at Ames Research Center in Moffett Field, CA, have both been excellent places to work and learn.

Dr. Bob Mahan, serving as my advisor for the past two years, has been an inspiration and a pleasure to work with. His enthusiasm, patience, and sense of direction, are greatly appreciated. I would also like to thank him for giving me the opportunity to work on such a fascinating project. I would also like to thank Dr. Curt Stern and Dr. Doug Nelson for serving on my thesis committee.

I would like to express thanks to Mr. Dennis Riddle, formerly of, and Mr. Clark White, of the STOVL/Powered-Lift Technology Branch, and Dr. Chuck Smith for their financial help with my graduate education. Thanks are also extended to Mr. Jim Lane, Branch Chief of the Military Technology Office, and Mr. Sam Wilson, Branch Chief of the STOVL/Powered-Lift Technology Branch, for their help with the

project.

I would also like to thank Mr. Glen Varney, Dr. Marc Cummings, and Ms. Pat Callahan of General Electric Aircraft Engines in Evandale, OH, for the opportunity to work with the infrared band model in the LOIR code. Special thanks are also extended to Mr. Pierre Villeneuve and Mr. Jeff Turk, fellow graduate students at VPI&SU, for their help with this project.

I would also like to thank Mr. Gary Hallock, Crew Chief of the Huey Helicopter, and of the Aircraft Services Branch, Dr. Merritt Smith of the Applied Computational Fluids Branch, Mr. Mike Stortz, Harrier Pilot, and of the Flight Operations Branch, and Mr. Alan Page of the Aircraft Systems Branch, all of NASA Ames, for their help with the infrared imaging of the Harrier YAV-8B flight tests.

I would like to express my thanks to Mr. Andy Hahn of the STOVL/Powered-Lift Technology Branch for his help with the Mackintosh Network system and software. I would also like to thank Mr. Torrie Stevens for patiently being my office mate and enduring the excess books and equipment in his office.

This work was conducted under NASA Ames grant NCC 2-691. I express thanks to all of the people who made that possible.

Finally, I would like to express sincere thanks to Dr. Larry Birckelbaw of the STOVL/Powered-Lift Technology Branch at NASA Ames. Larry has served as an excellent advisor and good friend while at Ames Research Center.

Sincere thanks are extended to my parents, Jim and Jean Nelson. They have provided a great deal of love and support. Thank you.

Table of Contents

Abstract	ii
Acknowledgements	iii
Table of Contents	vi
List of Illustrations	ix
List of Tables	xiii
Nomenclature	xiv
1.0 Introduction	1
2.0 Analytic Description of Infrared Band Model	6
2.1 Improvements to the NASA SP-3080 Band Model	6
2.2 Input Parameters to Program SAIL	7
2.3 Role of Program SAIL in CFD Code Validation	7
2.4 The Equation of Radiative Exchange	9

2.5 Calculation Procedure	10
2.5.1 STP Adjusted Path Length	10
2.5.2 Line Broadening	11
2.5.3 Doppler Half-Width	11
2.5.4 Collision Half-Width	12
2.5.5 Band-Averaged Absorption Coefficient	13
2.5.6 Line Density Parameters	14
2.5.7 Optical Depth for the Weak Line Limit	14
2.5.8 Doppler Broadened Fine Structure Parameter	16
2.5.9 Collision Broadened Fine Structure Parameter	16
2.5.10 Optical Depth for a Pure Doppler Curve of Growth	17
2.5.11 Optical Depth for a Pure Collision Curve of Growth	18
2.5.12 Combined Collision and Doppler Optical Depth	19
2.5.13 Optical Depth	19
2.5.14 Transmittance	20
2.6 SAIL Limitations	20
2.7 Summary of Assumptions in Program SAIL	21
3.0 Results	22
3.1 Band-Averaged Absorption Coefficient Improvements	22
3.2 Line Spacing Coefficient Improvements	24
3.3 Temperature Range Improvement	25

3.4 Comparisons among SAIL, SCORPIO, and LOIR	25
3.5 Comparison with AFRPL-TR-76-9	26
3.6 Computation Time	28
4.0 Conclusions and Recommendations	29
4.1 Conclusions	29
4.2 Recommendations	30
4.2.1 Test Facility Enhancements	30
4.2.2 Computational Fluid Dynamic (CFD) Activities	31
4.2.3 CFD Validation	31
4.2.4 Infrared Band Model Selection	32
Figures	34
Tables	67
References	71
Appendix A SAIL Sample Execution	76
Appendix B SAIL Sample Results	80
Appendix C SAIL Source Code Listing	83
Vita	108

List of Illustrations

Fig. 1.	Spectral response of Agema Thermovision® 880 medium wave length band infrared camera	35
Fig. 2.	Spectral response of Agema Thermovision® 880 long wave length band infrared camera	36
Fig. 3.	Photograph of the Agema Thermovision® 880 infrared imaging system	37
Fig. 4.	Infrared image composite of a Harrier YAV-8B in fly-by	38
Fig. 5.	Head on infrared image of a Harrier YAV-8B in hover condition.	39
Fig. 6.	Infrared image of an E7 supersonic STOVL prototype	40
Fig. 7.	Infrared image of an XV-15 Tiltrotor stationary on the runway .	41
Fig. 8.	Flow chart of Program SAIL	42
Fig. 9.	Attenuation of a band-limited beam of differential length du . .	43
Fig. 10.	A broadened spectral line	44
Fig. 11.	An example of the weak-line-limit model	45

Fig. 12.	An example of the strong-line-limit model	46
Fig. 13.	Comparison of the band-averaged absorption coefficient provided by NASA SP-3080 and Program SAIL for water vapor at 300 K.	47
Fig. 14.	Comparison of the band-averaged absorption coefficient provided by NASA SP- 3080 and Program SAIL for water vapor at 1200 K.	48
Fig. 15.	Comparison of the band-averaged absorption coefficient provided by NASA SP-3080 and Program SAIL for water vapor at 1800 K.	49
Fig. 16.	Comparison of the band-averaged absorption coefficient provided by NASA SP-3080 and Program SAIL for carbon dioxide at 300 K.	50
Fig. 17.	Comparison of the band-averaged absorption coefficient provided by NASA SP-3080 and Program SAIL for carbon dioxide at 1200 K	51
Fig. 18.	Comparison of the band-averaged absorption coefficient provided by NASA SP-3080 and Program SAIL for carbon dioxide at 1800 K	52
Fig. 19.	Comparison of the band-averaged absorption coefficient provided by NASA SP-3080 and Program SAIL for carbon monoxide at 300 K	53
Fig. 20.	Comparison of the band-averaged absorption coefficient provided by NASA SP-3080 and Program SAIL for carbon monoxide at 1200 K	54

Fig. 21.	Comparison of the band-averaged absorption coefficient provided by NASA SP-3080 and Program SAIL for carbon monoxide at 1800 K	55
Fig. 22.	Comparison of the line spacing coefficient provided by NASA SP-3080 and Program SAIL for water vapor at 600 K	56
Fig. 23.	Comparison of the line spacing coefficient provided by NASA SP-3080 and Program SAIL for carbon dioxide at 300 K	57
Fig. 24.	Comparison of the line spacing coefficient provided by NASA SP-3080 and Program SAIL for carbon monoxide at 300 K	58
Fig. 25.	An example of low temperature data provided by SAIL: transmittance of gas resembling the atmosphere	59
Fig. 26.	Comparison of results obtained using SAIL, LOIR, and SCORPIO for heated water vapor at low pressures	60
Fig. 27.	Comparison of results obtained using SAIL, LOIR, and SCORPIO for heated water vapor	61
Fig. 28.	Comparison of results obtained using SAIL, LOIR, and SCORPIO for heated carbon dioxide at low pressures.	62
Fig. 29.	Comparison of SAIL with AFRPL experimental data for isothermal hot water vapor at varying pressures. Temperature = 1177 K.	63
Fig. 30.	Comparison of SAIL with AFRPL experimental data for isothermal cold water vapor. Temperature = 296 K	64

Fig. 31. Comparison of SAIL with AFRPL experimental data for isothermal cold carbon dioxide. Temperature = 295 K. 65

Fig. 32. Comparison of SAIL with AFRPL experimental data for an isothermal cold mixture. Temperature = 297 K 66

List of Tables

Table 1.	Model values for the collision line width parameters	68
Table 2.	Example of the carbon dioxide band-averaged absorption coefficients	69
Table 3.	Example of the carbon dioxide line spacing coefficients	70

Nomenclature

Latin Symbols

$a_{c,n}$	Collision-Broadened Fine Structure Parameter (-)
$a_{D,n}$	Doppler-Broadened Fine Structure Parameter (-)
d_n	Distance Between Spectral Lines (cm^{-1})
$\frac{1}{d_n}$	Line Density Parameter, or Line Spacing Coefficient (cm)
$I_{\Delta\omega}$, $\Delta I_{\Delta\omega}$	Radiant Intensity Averaged Over Wavenumber Interval $\Delta\omega$ (W/Sr), Change in Radiant Intensity Across Path Length (W/Sr)
L , ΔL	Total Path Length (cm), Path Length of Volume Element (cm)
m_n	Molar Mass of n^{th} Constituent (kg/kmol)
P_n	Average Partial Pressure of n^{th} Constituent (atm)
T	Temperature (K)
Δu_n	STP-Adjusted Path Length (cm)
X	Optical Depth of the Mixture (-)
X_n	Optical Depth for the n^{th} Constituent (-)
$X_{c,n}$	Optical Depth for a Pure Collision Curve of Growth (-)
$X_{D,n}$	Optical Depth for a Pure Doppler Curve of Growth (-)
X_n^*	Optical Depth for the Weak Line Limit (-)

Y_n Combined Collision and Doppler Optical Depths (-)

Greek Symbols

$\gamma_{c,n}$ Collision Half-Width of n^{th} Constituent (cm^{-1})

$\gamma_{D,n}$ Doppler Half-Width of n^{th} Constituent (cm^{-1})

$(\gamma_{n,m})_{273}$ Foreign Collision-Broadening Constant Adjusted to STP Conditions (-)

$(\gamma_{n,n})_{273}$ Resonant Collision-Broadening Constant Adjusted to STP Conditions (-)

$\eta_{n,m}$ Factor for Temperature Correction of the Half-Width for Foreign Collision-Broadening (-)

$\eta_{n,n}$ Factor for Temperature Correction of the Half-Width for Resonant Collision-Broadening (-)

$\kappa, \bar{\kappa}$ Monochromatic Absorption Coefficient (cm^{-1}), Band Averaged Monochromatic Absorption Coefficient (cm^{-1})

τ Transmittance (-)

$\omega, \Delta\omega$ Wavenumber (cm^{-1}), Wavenumber Interval (cm^{-1})

1.0 Introduction

Joint research at the National Aeronautics and Space Administration (NASA) and Virginia Polytechnic Institute and State University (VPI&SU) has shown that infrared imaging can provide a validation technique for computational fluid dynamics (CFD) codes [1,2]. The validation technique involves a quantitative comparison between an experimental infrared image and a predicted infrared image, with the latter based on the CFD solution. Creating the predicted infrared image requires the use of an infrared band model. Infrared imaging and infrared band models are the topic of this thesis.

The aerodynamic flow field about a powered-lift aircraft operating in ground effect is difficult to model. This circulating flow field is characterized by a small forward velocity component and regions of supersonic to high subsonic jet flows. The recirculating flow can cause several effects including propulsion-induced loss of lift, or 'suck down,' ingestion of foreign objects or debris (FOD), and ingestion of warm, oxygen depleted, or vitiated, air [3-5]. Attempts to model these effects by conventional means, such as wind tunnel experiments, have been unsuccessful,

with the end result being that full-scale powered tests are required to study the actual flow field.

Extensive CFD research has been carried out in an attempt to correctly model the flow in ground effect in support of the design of future STOVL aircraft, see for example Refs. 6-8. Validation of the CFD code by infrared imaging of existing research aircraft reduces the need for costly full-scale experiments of candidate designs.

In recognition of the need for good infrared experimental data, an Agema Thermovision® Dual 880 Imaging System has been obtained and used for flow visualization as part of this research [9]. The imaging system is sensitive to two wavelength bands, 2.5 to 5.5 μm and 8 to 12 μm . Figures 1 and 2 show the response spectra of the two wavelength bands. The system scans a scene and digitally records the infrared image to a hard disk. A thorough technical discussion of the imaging system is available elsewhere [10,11]. Figure 3 shows the Agema Thermovision® Dual 880 infrared scanners, BRUT recording unit, color monitor and keyboard.

In the course of the work reported in this thesis, infrared imaging using the Agema Thermovision® 880 Dual System was successfully used to visualize gaseous flow about several powered-lift aircraft. These aircraft include the McDonnell-Douglas Harrier YAV-8B, the E7 supersonic STOVL prototype, and the XV-15 tiltrotor aircraft. The Agema infrared camera measures radiant intensity.

The different colors shown in Figures 4 through 7 represent bands of varying radiant intensity. Figures 4 and 5 show infrared images of the Harrier YAV-8B in different flight conditions. Figure 6 is an infrared image of the E7 supersonic STOVL prototype. Figure 7 is an infrared image of the XV-15 tiltrotor. Note from the figures that the intensity is greatest, shown in red and white, near the nozzle exit, decreases through the plume, and is finally lowest in the background.

It can be seen from Figures 4 through 7 that infrared imaging can provide a powerful means of flow visualization about a powered-lift aircraft. Also, the contributions by engine exhaust to ground heating and aircraft skin heating can also be seen. It is this ability to provide clear and accurate descriptions of the flow field which make infrared imaging a powerful resource for CFD code validation.

Prediction of an infrared image from a CFD solution is the final step in creating an image which can be compared directly to the experimental image. Creating an infrared image from the CFD solution requires knowledge of flow variables such as temperature, pressure, and species concentration at each node point in the solution. Calculating the emission and attenuation of radiation, given these flow variables, is the function of an infrared band model.

Over the past twenty years, considerable research has been done on infrared band models [12 - 16], and several commercial codes, see for example Refs. 17 through 18, and a few company proprietary codes, for example Ref. 19, are available. Each band model has its particular advantages. Comparisons of

results from different infrared band models are generally not available in the public-domain. Computation time and solution accuracy are important program features to be considered. For example, choosing a particular band model for the workstation environment is especially important when the goal is to provide a real-time user interface. Equally important is the selection of a band model to provide accurate, high-resolution images when a CRAY® or similar super computer is available.

In a previous study by Hardman [2], the heated exhaust flow from a free-jet apparatus based on an auxiliary power unit, was recorded using an infrared imaging system. A computer code was developed for converting the experimentally measured exhaust plume temperature distribution to the corresponding infrared image. It was demonstrated that a comparison between an experimental infrared image and an infrared image created from the measured temperature field has potential for use in verifying CFD codes. However, Hardman's computer model for predicting infrared emission neglected the effects of pressure. Also, the model did not include the contributions to infrared emission by participating gaseous constituents other than water vapor.

The primary motivation for this work is to satisfy the need for a public-domain infrared gaseous radiation model, of a quality equal to that of NIRATAM, which is tailored for CFD code validation. An infrared band model formulated by NASA and published in NASA SP-3080, the **Handbook of Infrared Radiation**

from Combustion Gases [20], has been coded and improved as part of the current research. The model has been improved by implementing data tables from the North Atlantic Treaty Organization (NATO) Infrared Air Target Model (NIRATAM) [18]. The resulting model is compared with other infrared band models.

This thesis describes an effort to better understand infrared imaging and infrared band models. The objective of future work will be to predict infrared images from CFD solutions. Prediction of the infrared images requires the use of an infrared band model. Chapter 2 describes the formulation of such a model. Each equation and concept is thoroughly explained. A computer code utilizing this methodology, Program SAIL (Selective Analytic Infrared Logic), has been developed and documented. Comparisons of this model with other infrared band models have been made and are the topic of Chapter 3. Finally, Chapter 4 concludes with a few recommendations for the future directions of this technology.

2.0 Analytic Description of the Infrared Band Model

The infrared band model which is the subject of this thesis is presented in this chapter. The discussion of the theory of this model follows largely from Chapter 5 of the **Handbook of Infrared Radiation from Combustion Gases**, NASA SP-3080 [20]. The analytical description is included here as an aid to the user of Program SAIL (Selective Analytic Infrared Logic). A sample execution of Program SAIL is given in Appendix A, and sample results are shown in Appendix B. Finally, a fully documented source code listing of Program SAIL is given in Appendix C.

2.1. Improvements to the NASA SP-3080 Band Model

The infrared band model presented in NASA SP-3080 and the infrared band model coded in SAIL, are fundamentally the same model. The equations are identical. The NASA SP-3080 band model and Program SAIL are statistical band models, as opposed to quantum-based, semi-empirical models. The data tables

in SAIL have been improved over the NASA SP-3080 band model, to provide five-wavenumber resolution over a broad wavenumber range, 400 to 5000 cm^{-1} (2 to 25 μm). The improved data tables were taken from the NATO Infrared Air Target Model (NIRATAM) source code [18].

2.2. Input Parameters to Program SAIL

The program is currently configured to compute the transmittance of a volume of gas of uniform temperature and pressure. Inputs to the program include:

1. Temperature
2. Pressure
3. Gaseous constituents present
4. Mole fraction of constituents
5. Path length
6. Wavelength, or wavenumber, range

Program SAIL is tailored for CFD code validation. Variables 1 through 4 in the list above are available from the CFD solution. Variables 5 and 6 are obtained as described in Section 2.3.

2.3. Role of Program SAIL in CFD Code Validation

Program SAIL has been tailored for CFD code validation. Recall that the validation technique involves a quantitative comparison between an experimental

infrared image, such as those shown in Figures 4 through 7, and an infrared image generated from the CFD solution using an infrared band model. Creating the latter image involves tracing a number of rays through the CFD solution domain. The ray-tracing technique reduces the three-dimensional solution space to a two-dimensional image, simulating the operation of a scanning infrared camera.

Each ray will be traced from infinity through the solution domain to the infrared camera. The radiant intensity arriving at the infrared camera along any given ray is a function of the gases through which that ray passes. Program SAIL evaluates the contribution of each individual volume element traversed by the ray.

The three-dimensional CFD solution space is comprised of nodes. At each node in the solution space, flow and field variables including temperature, pressure, and concentrations of the constituents present are available. At any point along the ray, an average value of these parameters may be computed from the values at the nodes bounding the volume element containing the point in question. These average values are then assumed constant in the volume element, an approximation which becomes increasingly valid as the size of the volume element decreases.

The radiant intensity arriving at the infrared camera along a given ray depends on the absorption and emission by each volumetric element along the ray. Program SAIL evaluates the contribution of a single volume element to this process.

2.4. The Equation of Radiative Exchange

The band-averaged radiant intensity arriving at some observer location U , is given by

$$I_{\Delta\omega}(\Delta\omega, U) = I_{\Delta\omega}(\Delta\omega, 0) e^{-X(\Delta\omega, U)} + \int_0^U I_{b, \Delta\omega}(\Delta\omega, T) \sum_n \left[\bar{\kappa}_n(\Delta\omega, T) e^{-(X_n(\Delta\omega, U) - X_n(\Delta\omega, u))} \right] du, \quad (1)$$

where $I_{\Delta\omega}(\Delta\omega, 0)$ is the radiant intensity in band $\Delta\omega$ at the beginning of the path, X is the optical depth of the path corresponding to physical position U , which is discussed in Section 2.5.13, $I_{b, \Delta\omega}(\Delta\omega, T)$ is the band-averaged blackbody distribution function, $\bar{\kappa}_n(\Delta\omega, T)$ is the band-averaged absorption coefficient of the n^{th} constituent, which is discussed in Section 2.5.5, and $X_n(\Delta\omega, U)$ is the contribution to the optical depth by the n^{th} constituent, which is discussed in Section 2.5.13. A derivation of the equation of radiative exchange may be found in Ref. 2 as well as in most radiation heat transfer textbooks.

Equation 1 explains how a volume along the path U may contribute to the radiant intensity arriving at the observer location. For example, if a ray of length U is traced from an arbitrary starting location a , to some observer location b , Equation 1 may be used to compute the radiant intensity arriving at location b . The radiant intensity at location a , $I_{\Delta\omega}(\Delta\omega, a)$, is attenuated along the path length U as described by the first term on the right-hand side of Equation 1. Emission and

absorption of radiation by volume elements along the path U , are computed by the second term on the right-hand side of Equation 1. Note that the contribution of each volume element is included by the integral over the path U . The contribution of each constituent to this process is included by the summation over n .

2.5. Calculation Procedure

The motivation of the procedure described in this section is to compute the optical depth X and the band-averaged absorption coefficient $\bar{\kappa}_n(\Delta\omega, T)$ for use in Equation 1. The equations required to compute these quantities are presented in the order that they are solved. Each equation shown in the development is solved in Program SAIL. Figure 8 shows a flow chart of Program SAIL.

Except as noted, the equations discussed in Sections 2.5.1 through 2.5.14 appear for the first time in Ref. 20, **Handbook of Infrared Radiation from Combustion Gases**. Each equation is explained in the context of this thesis. Some knowledge of fundamental gaseous radiation heat transfer and quantum theory is assumed in the development.

2.5.1. STP-Adjusted Path Length

The first task is to compute the path length of the volume element adjusted to Standard Temperature and Pressure (STP) conditions, Δu_n (cm). A different adjusted path length must be computed for each constituent, hence the subscript

n. The adjusted path length is given by,

$$\Delta u_n = \left(\frac{p_n}{1 \text{ atm}} \right) \left(\frac{273 \text{ K}}{T} \right) \Delta L , \quad (2)$$

where p_n is the partial pressure of the n^{th} constituent (atm), ΔL is the physical path length (cm), and T is the temperature across the segment (K).

2.5.2. Line Broadening

According to quantum theory, atoms and molecules occupy discrete, or quantum, energy states. As a result, only photons having discrete energy states may be absorbed or emitted. This gives rise to the appearance of absorption lines in the transmission spectrum. In principle these lines, called spectral lines, are infinitesimally thin; however, in reality they may be broadened by various physical phenomena, the two most important of which are described in Sections 2.5.3 and Sections 2.5.4. Figure 10 shows a broadened spectral line. Note that this line has a finite width and height.

2.5.3. Doppler Half-Width

The atoms or molecules of an emitting gas are not stationary, but move due to their thermal energy. When observed by a stationary observer, the frequency of emission of radiation of the moving molecule or atom may appear to increase or decrease, depending upon the velocity of the molecule relative to the observer.

This change of frequency is known as the Doppler effect, and it is this phenomenon which accounts for Doppler line broadening in infrared gaseous emission. Note that the molecules of a gas have a velocity distribution. Deviation from the mean velocity, both positive and negative, then gives rise to a finite spectral line width.

For a Doppler-broadened spectral line, the Doppler half-width, $\gamma_{D,n}$ (cm^{-1}), is the wavenumber interval from the line peak to the wavenumber corresponding to half the maximum line height. For the line model of Figure 10, the Doppler half-width is given by

$$\gamma_{D,n} = (5.94 \times 10^6) \frac{\omega}{m_n^{0.5}} \left(\frac{T}{273} \right)^{0.5}, \quad (3)$$

where T is the temperature of the volume element (K), m_n is the molar mass of the n^{th} constituent (kg/kmol), and ω is the wavenumber of the peak (cm^{-1}). This semi-empirical result, like many of those which follow in this chapter, is from Ref. 20.

2.5.4. Collision Half-Width

As the pressure of a gas is increased, the number of collisions an atom or molecule experiences also increases. These collisions can cause a perturbation in the energy states of the atom or molecule, resulting in spectral line broadening. This phenomenon is known as collision line broadening.

The collision half-width, γ_C (cm^{-1}), is the quantity in Program SAIL that takes

into account the effects of collision broadening. The collision half-width is the wavenumber interval from the line peak to the wavenumber corresponding to half the maximum line height. The collision half-width must be solved for each constituent n , but its value is a function of all other species m within the volume element. The collision half-width is given by

$$\gamma_{c,n} = \sum_m \left[(\gamma_{n,m})_{273} \rho_m \left(\frac{273}{T} \right)^{\eta_{n,m}} \right] + (\gamma_{n,n})_{273} \rho_n \left(\frac{273}{T} \right)^{\eta_{n,n}}, \quad (4)$$

where $(\gamma_{n,m})_{273}$ and $(\gamma_{n,n})_{273}$ are collision line-width parameters adjusted to STP conditions, and $\eta_{n,m}$ and $\eta_{n,n}$ are factors for temperature correction corresponding to the half-width. The quantities $(\gamma_{n,m})_{273}$ and $\eta_{n,m}$ correspond to collision broadening, or line broadening, of a species n due to the presence of a foreign species m , and $(\gamma_{n,n})_{273}$ and $\eta_{n,n}$ correspond to resonant collision broadening. Table 1 lists a selection of values for these parameters. Note from Table 1 that in the summation in Equation 4, m can be equal to n . Collision line broadening is discussed in several standard thermal radiation texts, for example Ref. 21.

2.5.5. Band-Averaged Absorption Coefficient

The monochromatic absorption coefficient, $\kappa_n(\omega, T)$ (cm^{-1}), is the property of the volume which describes the amount of absorption per unit path length within the volume. The monochromatic absorption coefficient averaged over band $\Delta\omega$

centered at ω , $\bar{\kappa}_n(\Delta\omega, T)$, is referred to as the band-averaged absorption coefficient. The band-averaged absorption coefficient is tabulated as a function of wavenumber and temperature for use in Program SAIL. Table 2, extracted from Ref. 18, lists typical values of $\bar{\kappa}_n(\Delta\omega, T)$ for carbon dioxide. These values must be read from a data file by Program SAIL. The full set of coefficients is available from the source code of Ref. 18.

2.5.6. Line Density Parameters

The line density parameter, or line spacing coefficient, $1/d_n$ (cm), where d_n (cm^{-1}) is a measure of the distance between spectral lines, is tabulated as a function of temperature and wavenumber for use in Program SAIL. Table 3, extracted from Ref. 18, lists some typical values for the line spacing coefficients for carbon dioxide. These values are read from a data file by Program SAIL. The full set of these coefficients is also available from the source code of Ref. 18.

2.5.7. Optical Depth for the Weak Line Limit

In order to describe the optical depth for the weak line limit we begin with an explanation of the terms *weak line limit* and *optical depth*. The weak line limit corresponding to a given species occurs when the line half-width is much larger than the line spacing; that is, when

$$\frac{\gamma}{d_n} \gg 1 . \quad (5)$$

In this limit the spectral lines are broad [22]. Figure 11 shows an example of the weak-line-limit model. Figure 12 shows an example of the strong-line-limit model for contrast.

The optical depth, $X(\Delta\omega, u)$, is the measure of a medium's ability to attenuate radiation. For example, a volume of gas with a large optical depth ($X \gg 1$) would appear opaque to incident radiation. Conversely, a volume with a small optical depth ($X \ll 1$) would appear transparent to incident radiation.

The optical depth for the weak line limit, X_n^* , is given by the integral over the path length,

$$X_n^* = \int_{\Delta u} \overline{\kappa}_n(\Delta\omega, T) du' . \quad (6)$$

For path lengths for which the band-averaged absorption coefficient, $\overline{\kappa}_n(\Delta\omega, T)$, may be considered constant over the path length, this integral is approximated by

$$X_n^* = \overline{\kappa}_n(\Delta\omega, T) \Delta u_n . \quad (7)$$

The optical depth for the weak-line-limit model is used in many of the following equations.

2.5.8. Doppler-Broadened Fine Structure Parameter

The fine structure parameters discussed in NASA SP-3080 are optical-path weighted, band-averaged ratios of the line width to line spacing. The Doppler-broadened fine structure parameter is given by the integral over the path length,

$$a_{D,n} = \frac{1}{X_n^*} \int_{\Delta u} \frac{\gamma_{D,n}}{d_n} \overline{\kappa}_n du' , \quad (8)$$

where $\gamma_{D,n}$ is the Doppler-broadened half-width. For path lengths where the integrand may be considered constant, the integral is approximated by

$$a_{D,n} = \frac{1}{X_n^*} \frac{\gamma_{D,n}}{d_n} \overline{\kappa}_n \Delta u_n . \quad (9)$$

Equation 9 may be simplified by introducing Equation 7, so that the Doppler-broadened fine structure parameter is given by

$$a_{D,n} = \frac{\gamma_{D,n}}{d_n} . \quad (10)$$

As discussed in Section 2.5.7, the relative size of this quantity with respect to unity is an indication of the applicability of the weak line limit for purely Doppler-broadened spectral lines.

2.5.9. Collision-Broadened Fine Structure Parameter

The collision-broadened fine structure parameter is given by the integral

over the path length,

$$a_{c,n} = \frac{1}{X_n^*} \int_{\Delta u} \frac{\gamma_{c,n}}{d_n} \overline{\kappa}_n du' , \quad (11)$$

where $\gamma_{c,n}$ is the collision-broadened half-width. For path lengths where the integrand may be considered constant, the integral is approximated by

$$a_{c,n} = \frac{1}{X_n^*} \frac{\gamma_{c,n}}{d_n} \overline{\kappa}_n \Delta u_n . \quad (12)$$

Equation 12 may also be simplified by introducing Equation 7, so that the collision-broadened fine structure parameter is given by

$$a_{c,n} = \frac{\gamma_{c,n}}{d_n} . \quad (13)$$

As discussed in Section 2.5.7, the relative size of this quantity with respect to unity is an indication of the applicability of the weak line limit for purely collision-broadened spectral lines.

2.5.10. Optical Depth for a Pure Doppler Curve of Growth

The description of the optical depth for a pure Doppler curve of growth begins with a discussion of the term *curve of growth*. As the path length of a ray increases, the band-averaged absorption of radiant energy along that path length also increases. The integral over wavenumber of the absorption, plotted as a

function of path length, defines the curve of growth. From this definition, the curve will always increase as the path length increases, hence the name *curve of growth*.

The optical depth for a pure Doppler curve of growth, X_D , is given by the empirical relation

$$X_{D,n} = 1.7 a_{D,n} \sqrt{\ln \left[1 + \left(\frac{X_n^*}{1.7 a_{D,n}} \right)^2 \right]} . \quad (14)$$

The quantity $X_{D,n}$ is used below in Equation 16.

2.5.11. Optical Depth for a Pure Collision Curve of Growth

The optical depth for a pure collision curve of growth, X_c , is given by

$$X_{c,n} = X_n^* \left[1 + \frac{X_n^*}{4 a_{c,n}} \right]^{0.5} . \quad (15)$$

The relative size of this quantity in comparison with $X_{D,n}$ reveals the relative importance of collision and Doppler line broadening. For example, if $X_{c,n} \gg X_{D,n}$, then collision broadening would be more important than Doppler broadening. This is most often the case in infrared gaseous radiation engineering calculations [21]. The optical depth for a pure collision curve of growth, $X_{c,n}$, is also used in Equation 16.

2.5.12. Combined Collision and Doppler Optical Depths

An intermediate step in computing the optical depth X , involves combining the collision and Doppler optical depths. The combination of the two quantities is accomplished by

$$Y_n = \left[1 - \left(\frac{X_{c,n}}{X_n^*} \right)^2 \right]^{-2} + \left[1 - \left(\frac{X_{D,n}}{X_n^*} \right)^2 \right]^{-2} - 1 . \quad (16)$$

The quantity Y_n is used in Equation 17 to compute the optical depth.

2.5.13. Optical Depth

The optical depth for an individual constituent, X_n , is a function of the optical depth for the weak line limit and the combined collision and Doppler optical depths, and is given by

$$X_n = \sqrt{1 - Y_n^{-0.5}} X_n^* . \quad (17)$$

The quantity X_n represents the contribution of an individual constituent to the optical depth of the volume element. The optical depth of the volume element, X , is given by the summation over the contributions of each of the constituents present, that is,

$$X = \sum_n X_n . \quad (18)$$

The optical depth is a key component to computing the attenuation of radiant energy by a volume element, as can be seen from the equation of radiative exchange, Equation 1. The reader should note that the optical depth X is a band-averaged quantity.

2.5.14. Transmittance

The band-averaged transmittance of a volume of gas is defined as the ratio of radiant energy leaving the volume to the radiant energy entering the volume in band $\Delta\omega$. The transmittance, τ , is related to the optical depth by

$$\tau = \exp(-X) . \quad (19)$$

A discussion of transmittance may be found in many gaseous radiation texts, for example Ref. 21.

2.6. SAIL Limitations

Some limitations are inherent in the current version of Program SAIL due to the limited availability of data. The band-averaged absorption coefficients and line spacing coefficients are available from the source code of Ref. 18 for water vapor, carbon dioxide, and carbon monoxide. These coefficients are tabulated from 400 to 5000 cm^{-1} at 5 cm^{-1} intervals for temperatures of 100, 200, 300, 600, 1200, 1800, 2400 and 3000 K.

2.7. Summary of Assumptions in Program SAIL

Several assumptions are made in computing the attenuation of radiant energy through a volume of gas. The assumptions are summarized here for completeness.

1. It is assumed that there is no scattering of radiation by particles or molecules in the volume element.
2. It is assumed that the volume element is isotropic; the properties of the volume element are independent of direction, or angle.
3. The volume element is assumed to be in local thermodynamic equilibrium; thus thermodynamic properties such as temperature and pressure can be used to describe the state of the volume element.
4. Radiative equilibrium is assumed. As a consequence, the volume element emits radiation at the same rate as radiation is absorbed.
5. Kirchoff's law is assumed to be valid. For radiative equilibrium, the monochromatic radiation absorbed equals the monochromatic radiation emitted. That is, radiative equilibrium is assumed at each wavelength.
6. Radiation within the volume element is assumed to be coherent; induced emission is radiated at the same wavelength of the incident radiation.

3.0 Results

Results of the infrared band model implemented in Program SAIL are presented in this chapter. Improvements to the band-averaged absorption coefficient and line spacing coefficient have been made to those published in NASA SP-3080, and results illustrating this improvement are given. Also shown are comparisons with results from other infrared band models, namely the band models contained in SCORPIO [24] and LOIR [19]. Results are also compared with experimental data published by the Air Force Rocket Propulsion Laboratory (AFRPL) [23].

3.1. Band-Averaged Absorption Coefficient Improvements

Recall that the monochromatic absorption coefficient averaged over band $\Delta\omega$ centered at ω , $\bar{\kappa}_n(\Delta\omega, T)$ (cm^{-1}), is tabulated as a function of temperature and wavenumber for use in Program SAIL. The resolution of the band-averaged absorption coefficients for water vapor, carbon dioxide, and carbon monoxide have been improved over those previously published in Ref. 20. The resolution published in Ref. 20 varied from 5 to 25 cm^{-1} , depending upon the constituent and

the position within the spectrum. The resolution provided in SAIL is 5 cm^{-1} and coefficients are listed from 400 to 5000 cm^{-1} .

Recall that the improved band-averaged absorption coefficients and line spacing coefficients available in SAIL, were extracted from the source code of Ref. 18. The improved coefficients come from comparisons with line-by-line calculations and experimental data. According to Cornet [25], for those coefficients corresponding to a temperature of 600 K or less, the values have been improved by comparisons with an Air Force line-by-line data base and for those values greater than 600 K, the coefficients were improved by a comparisons with experimental data.

A comparison of these coefficients with coefficients published in Ref. 20 is given in Figures 13 through 21. Figures 13 through 15 show a comparison between water vapor coefficients in SAIL and those from Ref. 20 for temperatures of 300, 1200, and 1800 K, respectively. Figure 13 shows a great deal of resolution enhancement, while Figures 14 and 15 show little significant improvement of SAIL over NASA SP-3080. Figures 16 through 18 show similar comparisons for carbon dioxide at the same three temperatures. The three fundamental bands of absorption for carbon dioxide can be identified from these figures. They are 3700 cm^{-1} ($2.7\text{ }\mu\text{m}$), 2325 cm^{-1} ($4.3\text{ }\mu\text{m}$), and 666 cm^{-1} ($15\text{ }\mu\text{m}$). No significant improvements are noticeable here; however, the agreement with the band-averaged absorption coefficients published in Ref. 20 is good across the infrared

spectrum, 400 to 5000 cm^{-1} (2 to 25 μm). Figures 19 through 21 give comparisons of these coefficients for carbon monoxide at the same three temperatures. The resolution has been significantly improved over that of Ref. 20 for each of the three temperatures studied. Note from Figures 19 through 21 that the magnitude of the absorption coefficient decreases with increasing temperature. Also, note that the width of the absorption band increases with increasing temperature. These trends are expected due to collision line broadening, as explained in Section 2.5.4. This phenomenon is discussed more fully in Ref. 21.

3.2. Line Spacing Coefficient Improvements

Recall that the line density parameter, or line spacing coefficient, $1/d_n$ (cm), where d_n (cm^{-1}) is a measure of the distance between spectral lines and is tabulated as a function of temperature and wavenumber for use in Program SAIL. The resolution has been improved over the resolution previously published in Ref. 20 and is shown in Figures 22 through 24. Figure 22 shows a comparison between the line spacing coefficients for water vapor at 600 K provided in Ref. 20 and those provided in SAIL. The comparison shows a significant improvement in the resolution across the infrared spectrum. Figure 23 shows a similar improvement for carbon dioxide. The 2325 cm^{-1} (4.3 μm) band is shown here. Figure 24 shows a significant improvement for carbon monoxide in its primary absorption band, 1960 to 2230 cm^{-1} (4.48 - 5.10 μm). In fact, the coefficients from

Ref. 20 seem to be substantially in error.

3.3. Temperature Range Improvement

The improved band-averaged absorption coefficients and line spacing coefficients in SAIL are available in a wide range of temperatures. Data are available at 100, 200, 300, 600, 1200, 1800, 2400, and 3000 K. With the improved coefficients in the lower temperature ranges, namely 100 K through 300 K, a typical atmospheric gas can be modeled by Program SAIL. Figure 25 shows the absorptivity as a function of wavenumber for dry air at a temperature of 285 K. Note that the only absorbing constituent present is carbon dioxide and that the three fundamental bands of carbon dioxide are visible from the figure. The other gases present, namely nitrogen and oxygen, do not absorb radiation, but act to broaden the absorption of carbon dioxide.

3.4. Comparisons among SAIL, SCORPIO, and LOIR

SCORPIO is an infrared band model created and used by General Electric Aircraft Engines. LOIR is not a band model, but it contains a band model derivative of SCORPIO. For simplicity, the band model in LOIR is referred to here as LOIR. The results of SAIL have been compared with results from SCORPIO and LOIR, and those results are shown in Figures 26 through 28. Figure 26 shows a comparison of the three models for heated water vapor at low pressure.

In this example, SAIL provides a much higher degree of resolution than do the other models. Also note that the general trends of the three models are similar. Figure 27 shows a similar comparison for heated water vapor at near atmospheric pressure. In this figure there is not a significant improvement in the resolution, and the trends of the three models are similar. Finally, Figure 28 shows a comparison between the three models for heated carbon dioxide. Note that the LOIR curve is shifted to the right relative to the other two models. Also note that the shape of SAIL is significantly different from that of the other two models, but that there is no significant increase in spectral resolution provided by SAIL over the other two models.

3.5. Comparison with AFRPL-TR-76-9

The Air Force Rocket Propulsion Laboratory (AFRPL) has published an assessment of the NASA band model [23]. The assessment concludes that for mixtures of water vapor, carbon dioxide, and other gases (namely, nitrogen, carbon monoxide, and hydrogen), the agreement with experimental data is 'good.' However, some problems are noted when pure carbon dioxide is modeled. The assessment concludes that the band model parameters for pure carbon dioxide appeared to be in error. The experimental data have been digitally extracted from Ref. 23 and compared to results obtained using SAIL. The digital extraction involved digitizing the graphs from a copy of the report, displaying the digitized

image on a computer screen, and using Digimatic® software to identify the origin, axes, and corresponding data points of the graph. By this process, the data from an x-y plot in a printed report can be extracted and saved to a data file. All of the SAIL results, including those modeling pure carbon dioxide, appear to be in good agreement with the Air Force data, indicating an improvement over the NASA SP-3080 model.

Figure 29 shows a comparison of SAIL with the AFRPL experimental data for isothermal hot water vapor at varying pressures for a temperature of 1177 K. SAIL follows the trends of the experimental data for each of the three pressures shown. However, the predicted absorptivity appears to be somewhat higher than the AFRPL measurements at each of the three pressures. Figure 30 shows a comparison between SAIL and experimental data for isothermal cold water vapor at a temperature of 296 K. While SAIL offers a much higher degree of resolution than that offered by the experimental data, the general trend of the two curves is the same. Note from Figure 30 that an absorption line coincides with nearly all of the experimental data points.

Recall that the AFRPL report, in its assessment of the NASA SP-3080 band model, concluded that there appear to be errors with modeling pure carbon dioxide [24]. Figure 31 shows a comparison of SAIL results with AFRPL experimental data for cold carbon dioxide at a temperature of 295 K. The curve matches the experimental data almost perfectly for the 3700 cm^{-1} ($2.7\text{ }\mu\text{m}$) band. The error

discussed in Ref. 23 seems to have been corrected with the updated absorption and line spacing coefficients. Figure 32 shows a comparison of SAIL with AFRPL experimental data for an isothermal cold mixture of water vapor, carbon dioxide, and nitrogen at 297 K. This figure also demonstrates good agreement between the SAIL model and the experimental data.

3.6. Computation Time

Execution time of Program SAIL is very short. For example, 1.5 CPU-seconds was required on a DIGITAL VAXstation® 2000 to generate the data for Figure 32. The VAXstation® 2000 is a 0.8 VAX unit of performance (VUP) machine. This time excludes reading and writing operations, as well as user interaction time. These operations are time-intensive operations, and so for repetitive use of Program SAIL these operations are minimized.

4.0 Conclusions and Recommendations

4.1. Conclusions

1. Infrared imaging using an Agema Thermovision[®] 880 Dual System has been successfully used to visualize gaseous flow about three powered-lift aircraft. These aircraft are the McDonnell-Douglas Harrier YAV-8B, the E7 supersonic STOVL prototype, and the XV-15 tiltrotor aircraft.
2. A FORTRAN computer code, Program SAIL, has been developed using the logic described in NASA SP-3080. The code can be used to model the emission of the three predominant emitting gases in the infrared: carbon dioxide, water vapor, and carbon monoxide.
3. Improvements of the band model published in NASA SP-3080, provided in Program SAIL, have been demonstrated. The resolution of the band-averaged absorption coefficients and line spacing coefficients for water vapor, carbon dioxide, and carbon monoxide has been increased to 5 cm^{-1} . The range over which the coefficients are listed has also been increased to include data from 400 cm^{-1} to 5000 cm^{-1} .

4. The results of Program SAIL have been compared with other infrared band models and with experimental data published by the Air Force Rocket Propulsion Laboratory (AFRPL). These comparisons establish Program SAIL as a viable tool for predicting monochromatic attenuation of radiation through exhaust gases and the atmosphere.
5. The success with infrared imaging of STOVL aircraft and predicting monochromatic attenuation through atmospheric and jet plume gases demonstrated in this thesis establishes the feasibility of CFD code validation based on infrared imaging of aircraft.

4.2. Recommendations

The primary goal of this thesis was to develop an infrared band model for computational fluid dynamic code (CFD) validation. Such an infrared band model code has been formulated and tested. The following recommendations are made for the next phase of this work, which is to adapt this technology to CFD code validation. This work is proposed as the author's doctoral dissertation topic.

4.2.1. Test Facility Enhancements

In an earlier effort (see Ref. 2) an auxiliary power unit (APU) was modified to provide a known heated exhaust temperature and velocity profile. The exhaust from this plume was experimentally imaged, and an analytic model for creating an infrared image from the temperature profile was used to generate an infrared

image for comparison with the experimental infrared image. It is proposed that this effort be duplicated, with the following changes. In addition to infrared imaging of the APU exhaust plume, the experiments should also be modeled using an existing CFD code [27] and the SAIL code. The APU can be tested with different nozzle shapes and varying exit conditions. Possible scenarios include:

- (a) Flow from a rectangular nozzle impinging on a flat plate to simulate current two-dimensional thrust vectoring nozzles.
- (b) Flow from a circular nozzle impinging on a flat plate to simulate current upper surface blowing (USB) configurations.
- (c) Flow from a circular nozzle impinging on an instrumented flat plate to simulate STOVL hover conditions.

4.2.2. Computational Fluid Dynamic (CFD) Activities

The test scenarios described above should be modeled by existing CFD codes [27]. The results of these codes would include a description of the temperature field, pressure distribution, and species concentration downstream of the nozzle exit. These results would be used in conjunction with the infrared band model developed in this thesis to create an infrared image.

4.2.3. CFD Validation

The proposed CFD validation technique involves a quantitative comparison

between an experimental infrared image and an infrared image created from the CFD solution. Reducing the three-dimensional CFD solution to a two-dimensional infrared image involves a ray-tracing technique through the generalized CFD solution domain, as well as the use of an infrared band model to relate field and flow variables to infrared emission. The ray-tracing technique should be robust to accommodate multiple overlapping grids, high density gradients, and solid surfaces.

The ray-tracing technique would involve scanning a generalized solution domain much like the infrared imaging system scans a scene. The radiant intensity arriving at each pixel on the image due to a ray would depend on the absorption and emission of radiation by the gases through which that ray passes.

The infrared image created from the CFD solution and the infrared image from the experiment would then be compared. This step would involve a pixel-by-pixel comparison in an image-processing computer environment. The quantitative comparison between the two images would then be used to validate CFD codes.

4.2.4. Infrared Band Model Selection

Different infrared band models are available offering varying degrees of accuracy throughout the infrared spectrum. The accuracy of these band models and the speed at which they compute attenuation are two parameters subject to

optimization for use in CFD validation. The LOWTRAN code [17] should be used to model the attenuation of radiant energy through the atmosphere surrounding an engine exhaust plume. It is proposed to use the SAIL code to model the attenuation through and emission from an engine exhaust plume. The infrared band model for a given region within a CFD solution should be chosen to give the appropriate degree of accuracy at the lowest computational expense.

Figures

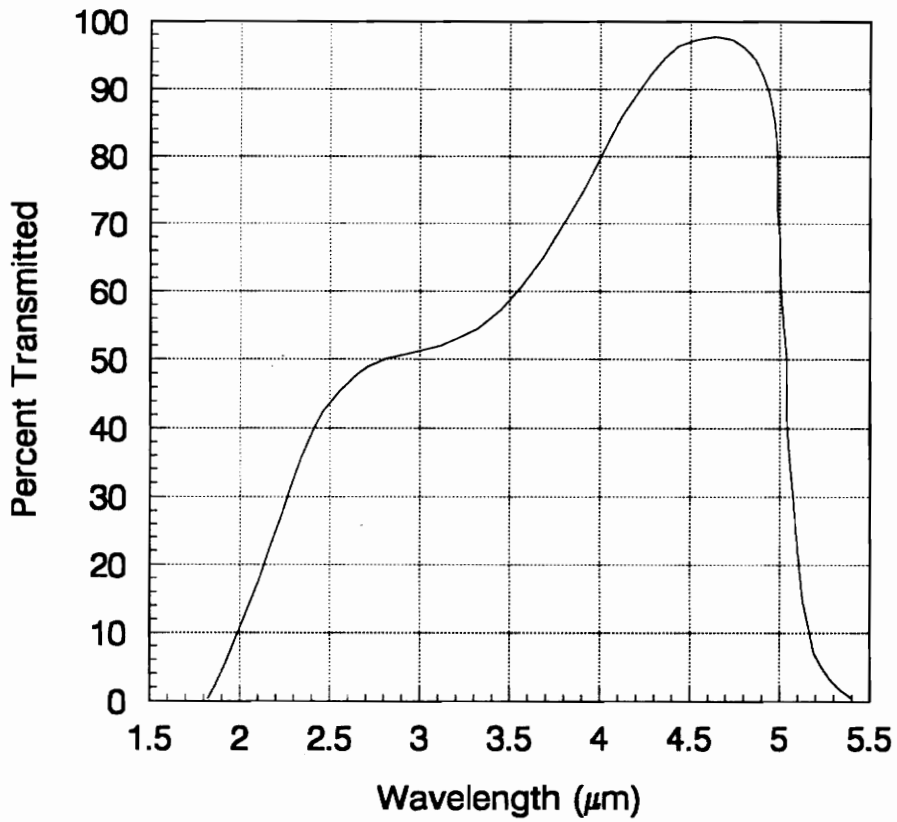


Figure 1. Spectral response of the Agema Thermovision® 880 medium wavelength band camera [26].

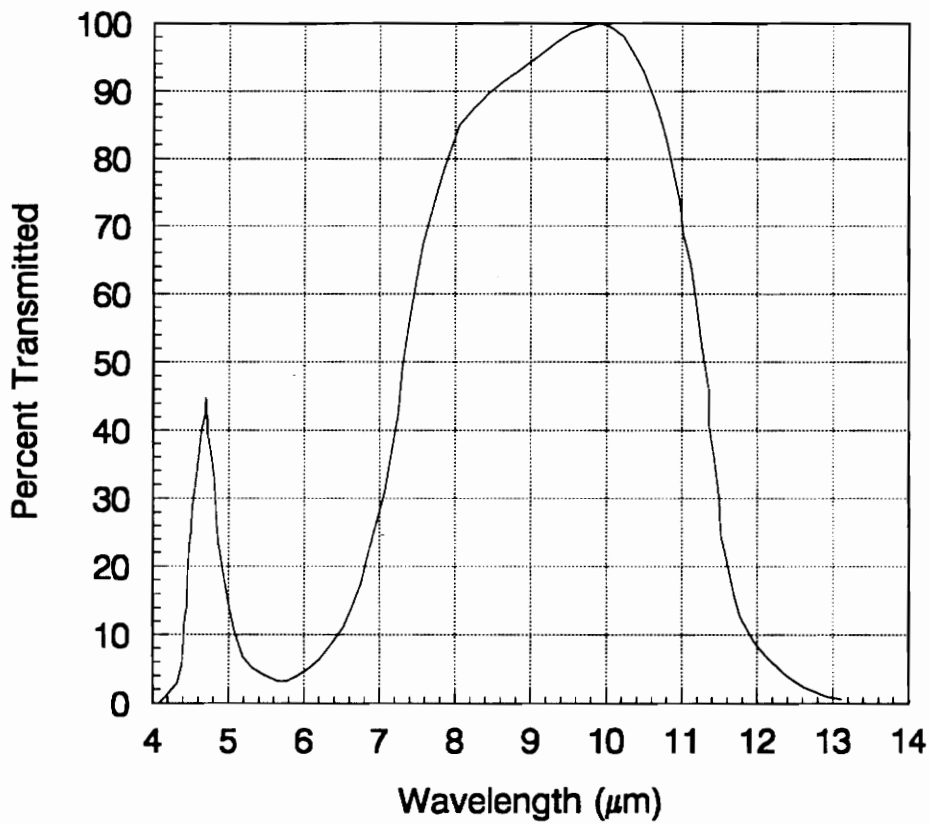


Figure 2. Spectral response of the Agema Thermovision[®] 880 long wavelength band camera [26].

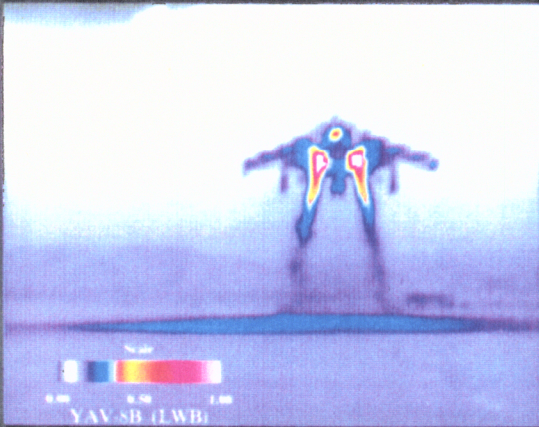
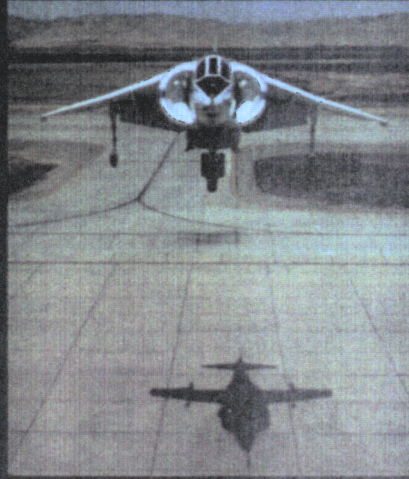


Figure 3. Photograph of the Agema Thermovision[®] 880 infrared imaging system showing the processing unit, color monitor, keyboard, and infrared scanners.



Figure 4. Infrared image composite of a Harrier YAV-8B in fly-by. The most intense areas are shown in red and white and are near the center of the aircraft. Radiant energy is scattered by dust from the runway in the top right image.

Infrared Imaging of Harrier YAV-8B



Code FAP: L. Birckelbaw, E. Nelson

Figure 5. Head-on infrared image of a Harrier YAV-8B in hover condition. Both infrared images are in the long wavelength band (8 - 12 μm). The most intense areas are shown in red and white and are near the center of the aircraft. Note the heating of the ground by the exhaust plumes.

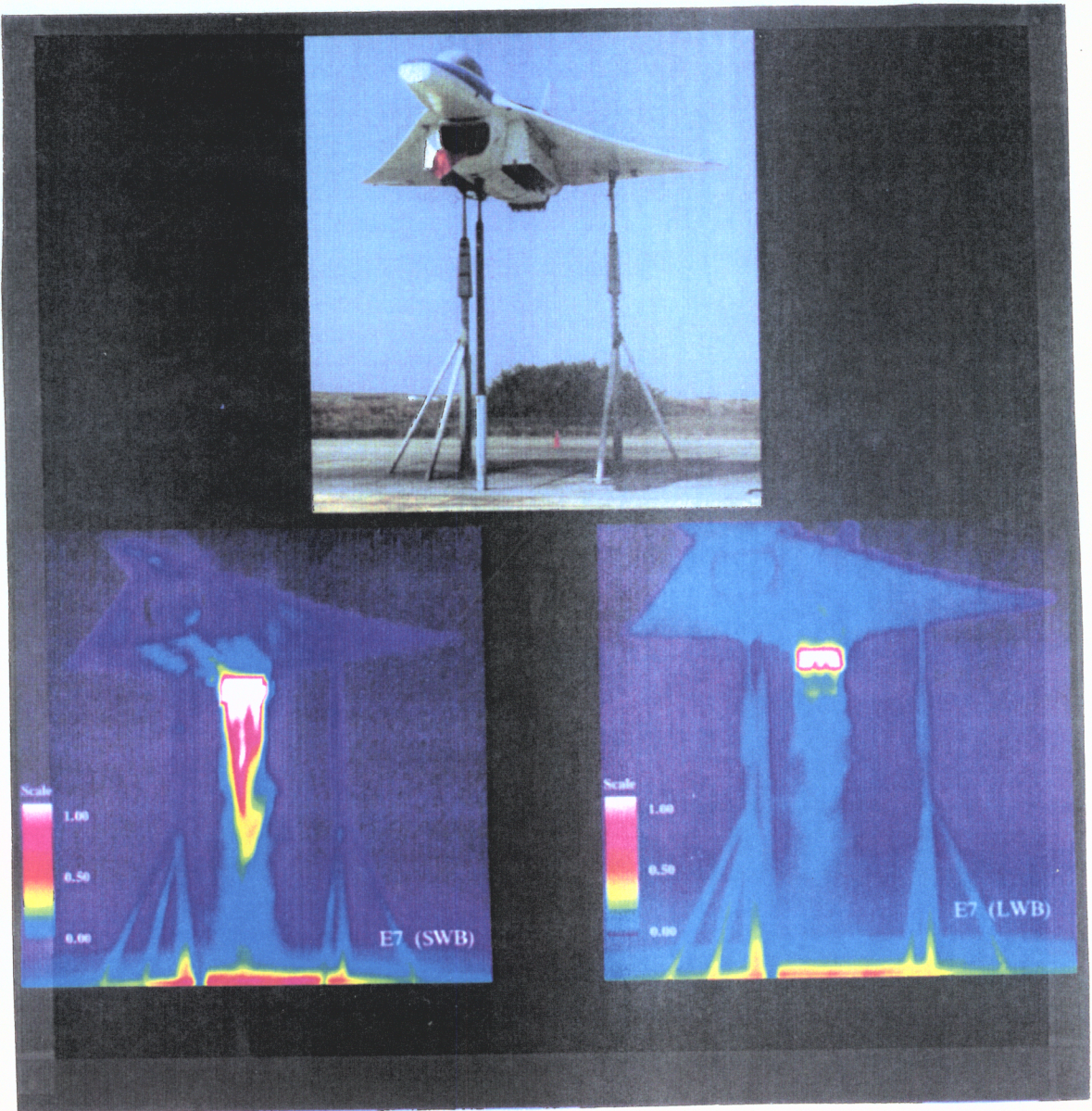


Figure 6. Infrared image of an E7 Supersonic STOVL prototype. The image on the lower left is for the medium wavelength band (MWB) (3 - 5 μm). The image on the lower right is for the long wavelength band (LWB) (8 - 12 μm). Note the dramatic difference in the intensity of the plume between the MWB and LWB images.



Figure 7. Infrared image of an XV-15 Tiltrotor stationary on the runway. Note the ground heating from the impinging jet engine exhaust plumes. The intense spot on the windshield in the lower left image is due to solar reflection.

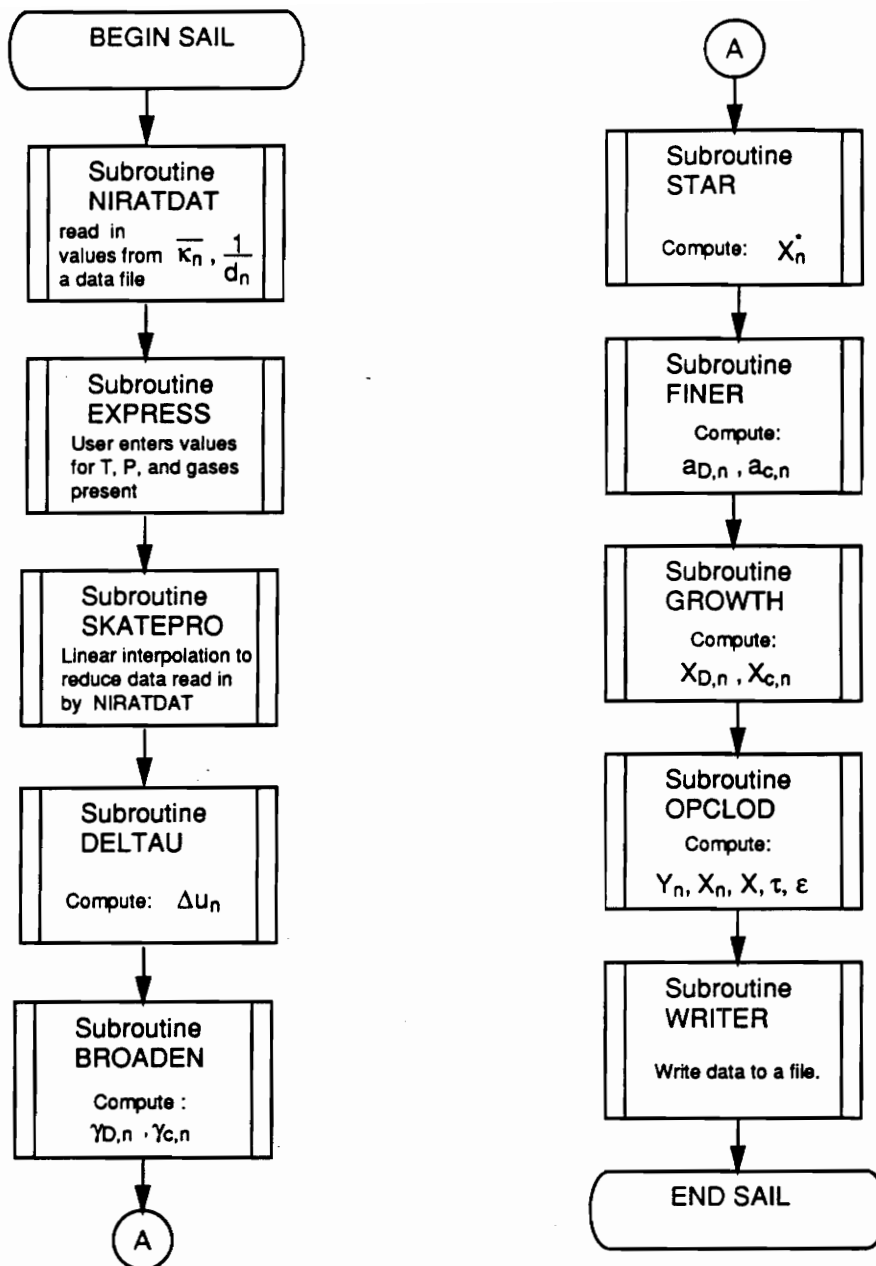


Figure 8. Flow chart of Program SAIL.

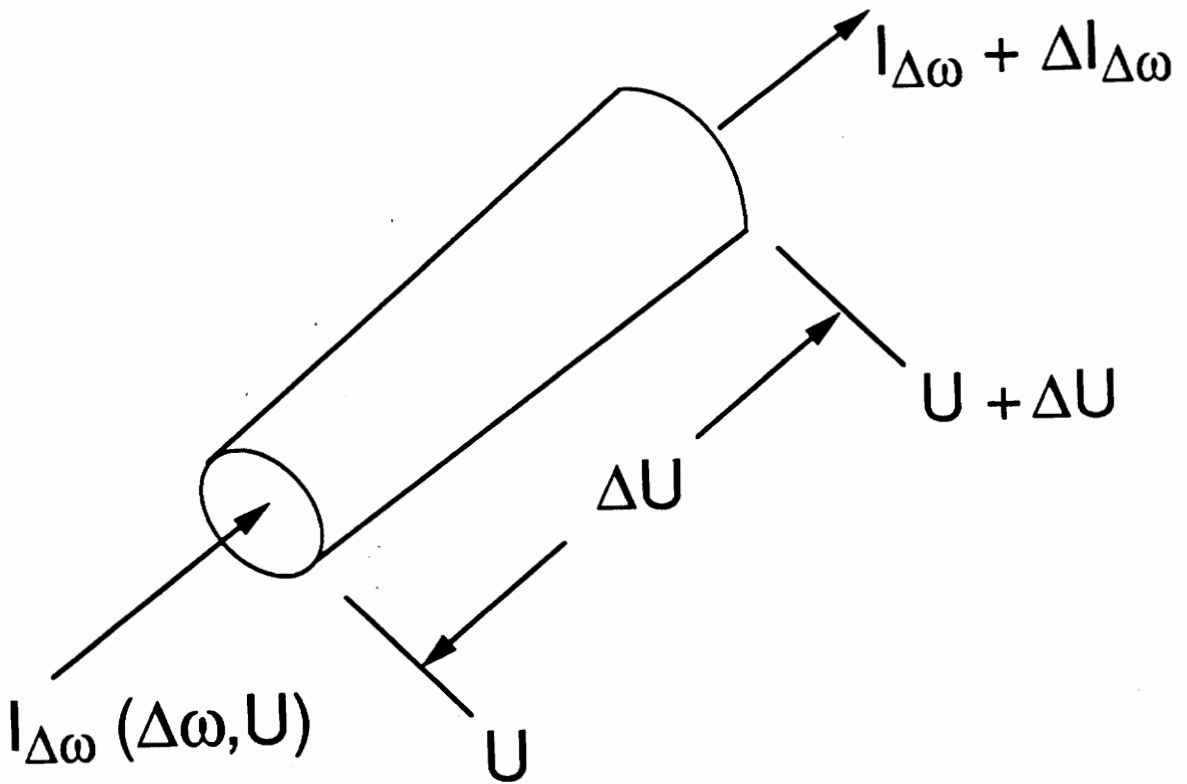


Figure 9. Attenuation of a band-limited beam of differential length du .

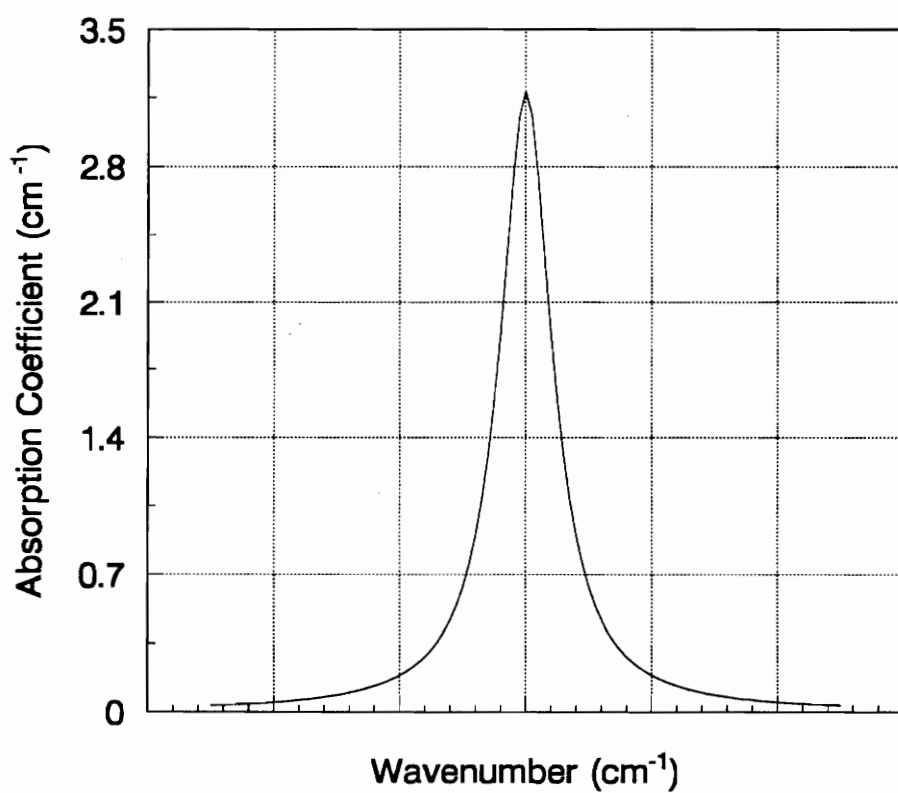


Figure 10. A broadened spectral line.

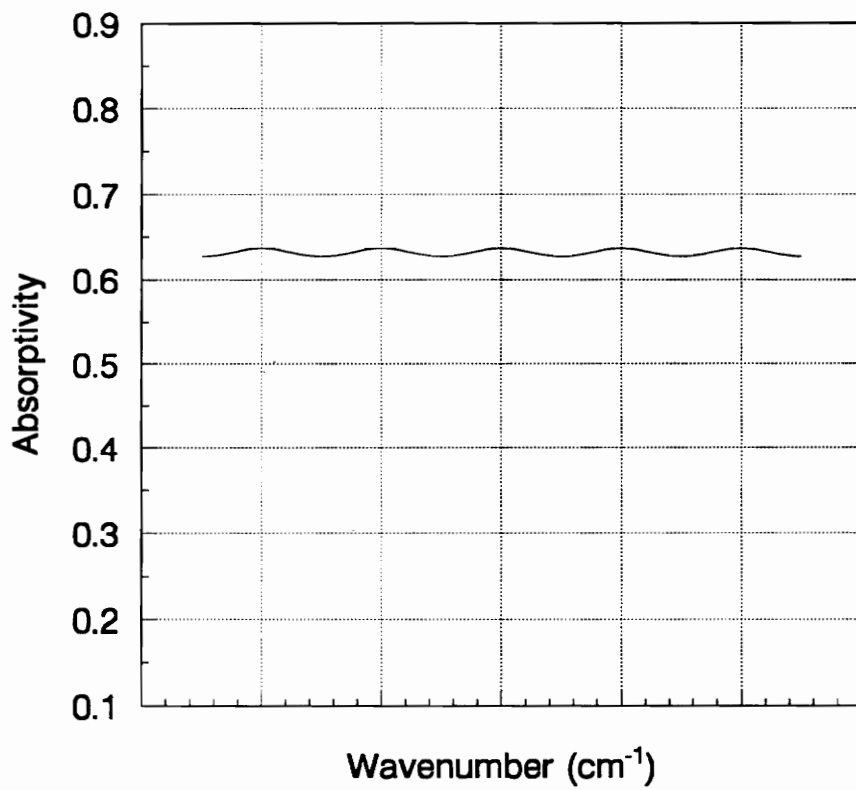


Figure 11. Illustration of the weak-line-limit model (level is arbitrary).

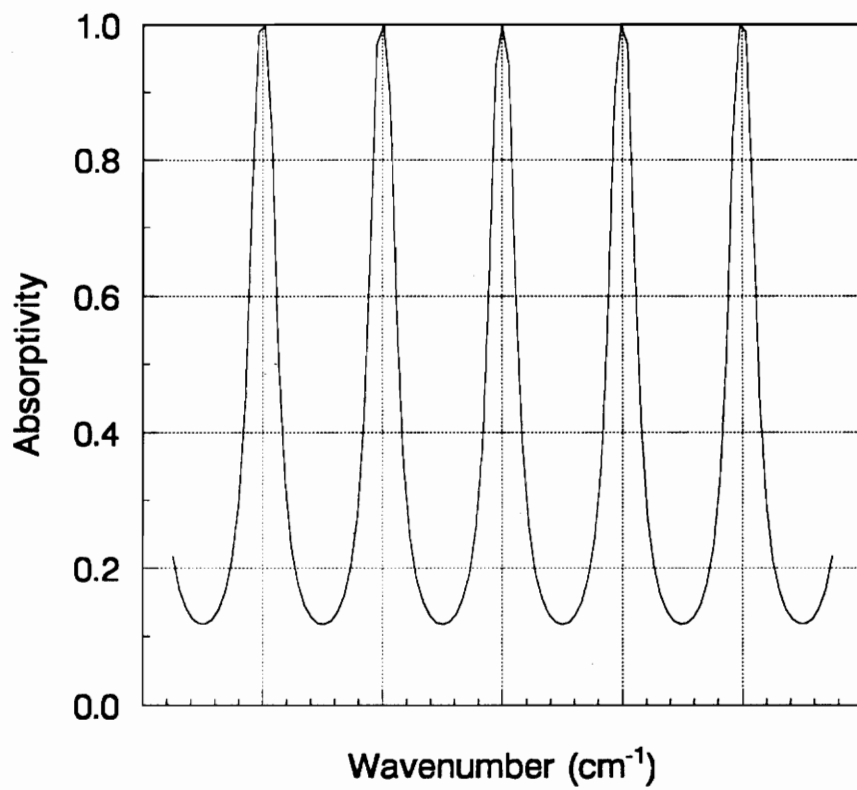


Figure 12. Illustration of the strong-line-limit model.

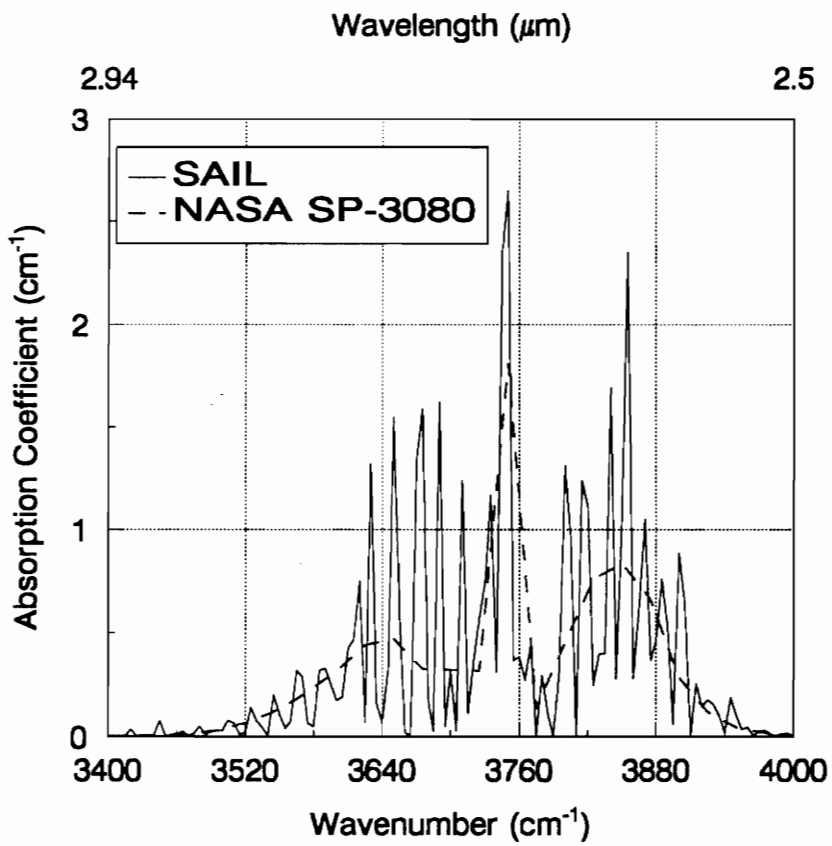


Figure 13. Comparison of the band-averaged absorption coefficient provided by NASA SP-3080 and Program SAIL for water vapor at 300 K.

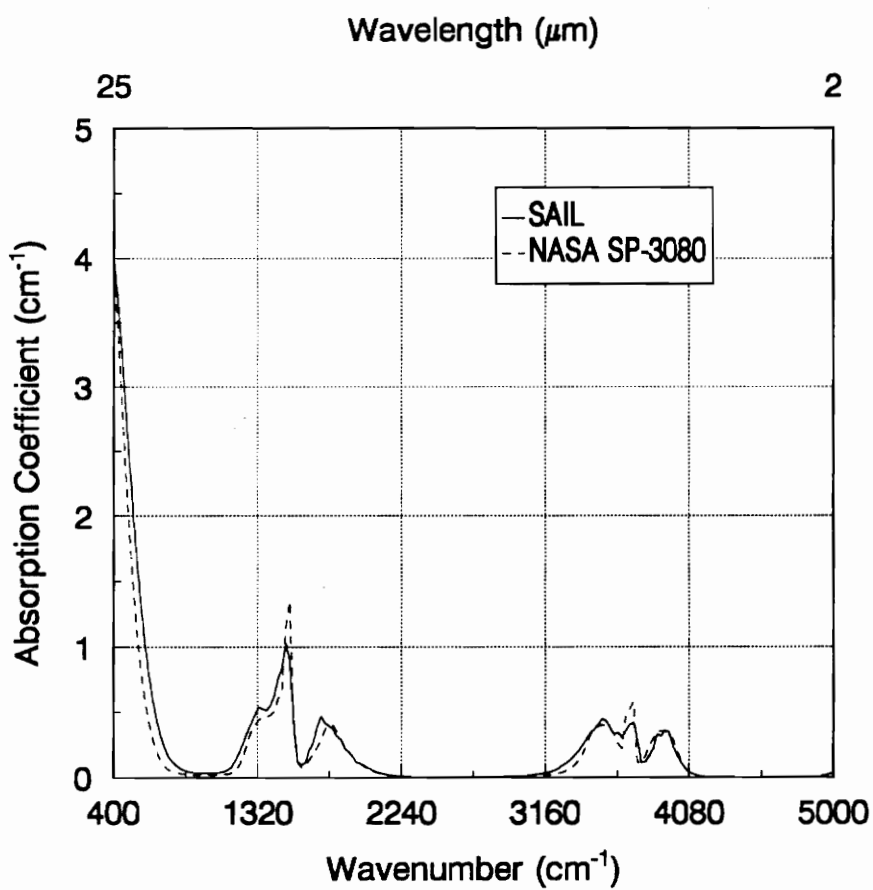


Figure 14. Comparison of the band-averaged absorption coefficient provided by NASA SP-3080 and Program SAIL for water vapor at 1200 K.

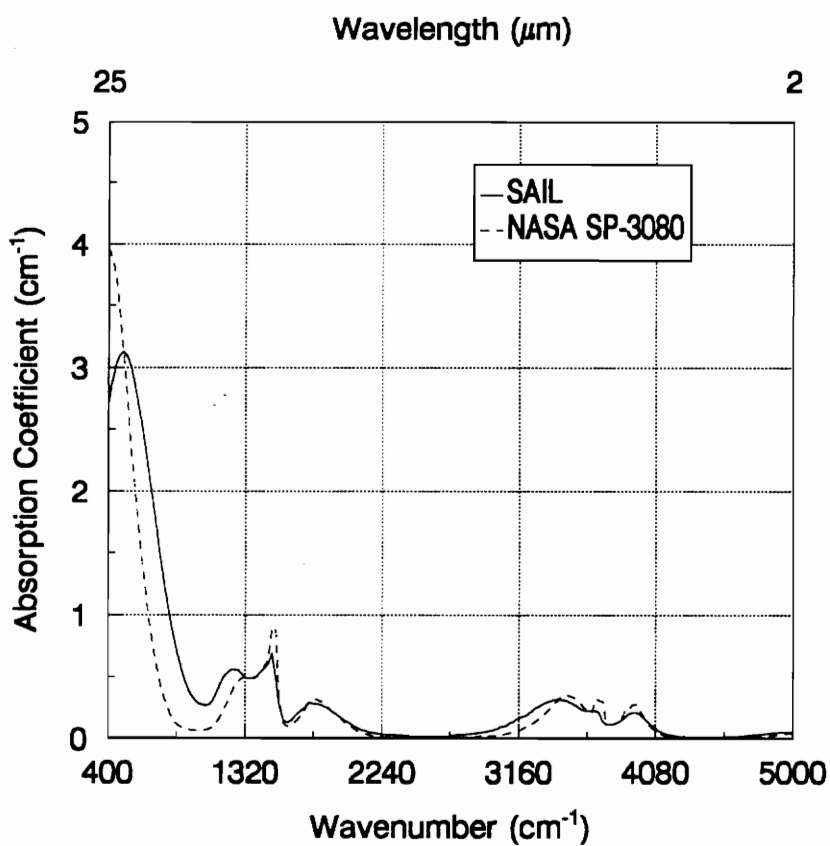


Figure 15. Comparison of the band-averaged absorption coefficient provided by NASA SP-3080 and Program SAIL for water vapor at 1800 K.

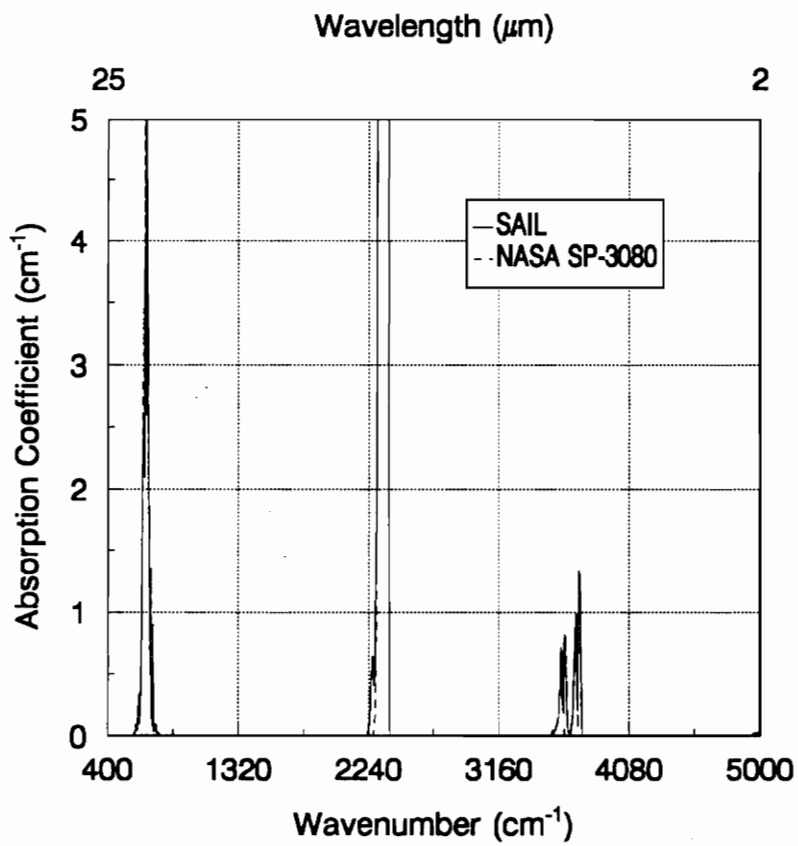


Figure 16. Comparison of the band-averaged absorption coefficient provided by NASA SP-3080 and Program SAIL for carbon dioxide at 300 K.

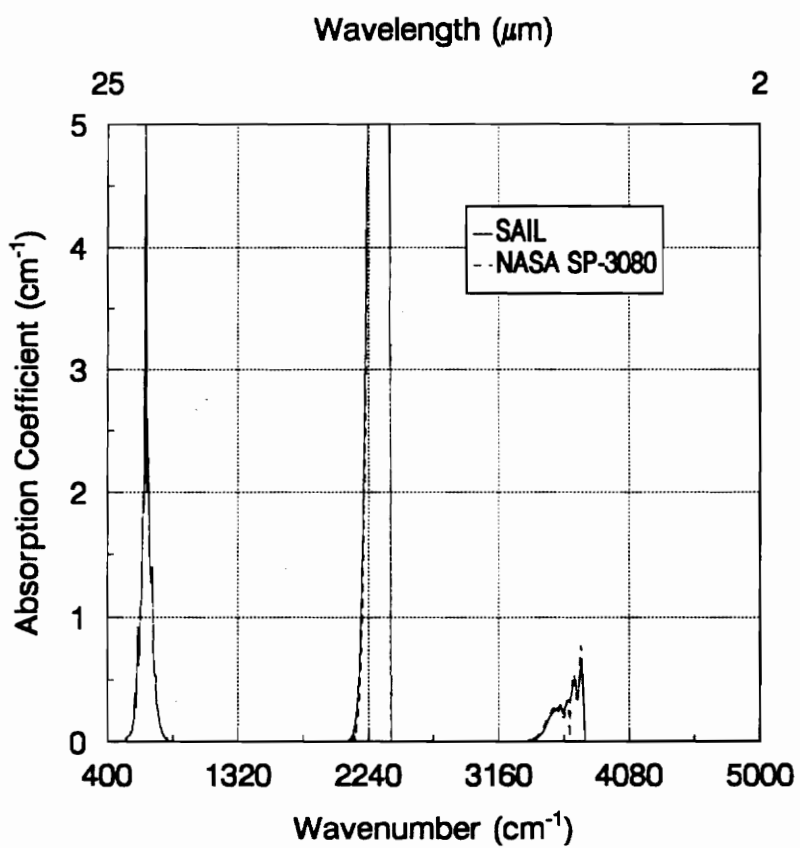


Figure 17. Comparison of the band-averaged absorption coefficient provided by NASA SP-3080 and Program SAIL for carbon dioxide at 1200 K.

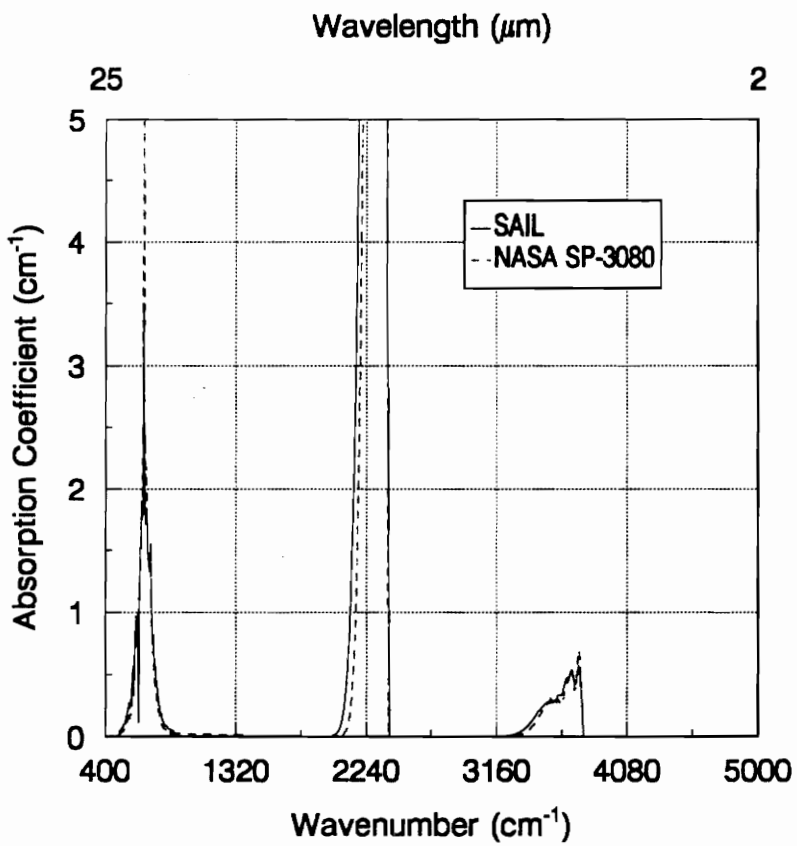


Figure 18. Comparison of the band-averaged absorption coefficient provided by NASA SP-3080 and Program SAIL for carbon dioxide at 1800 K.

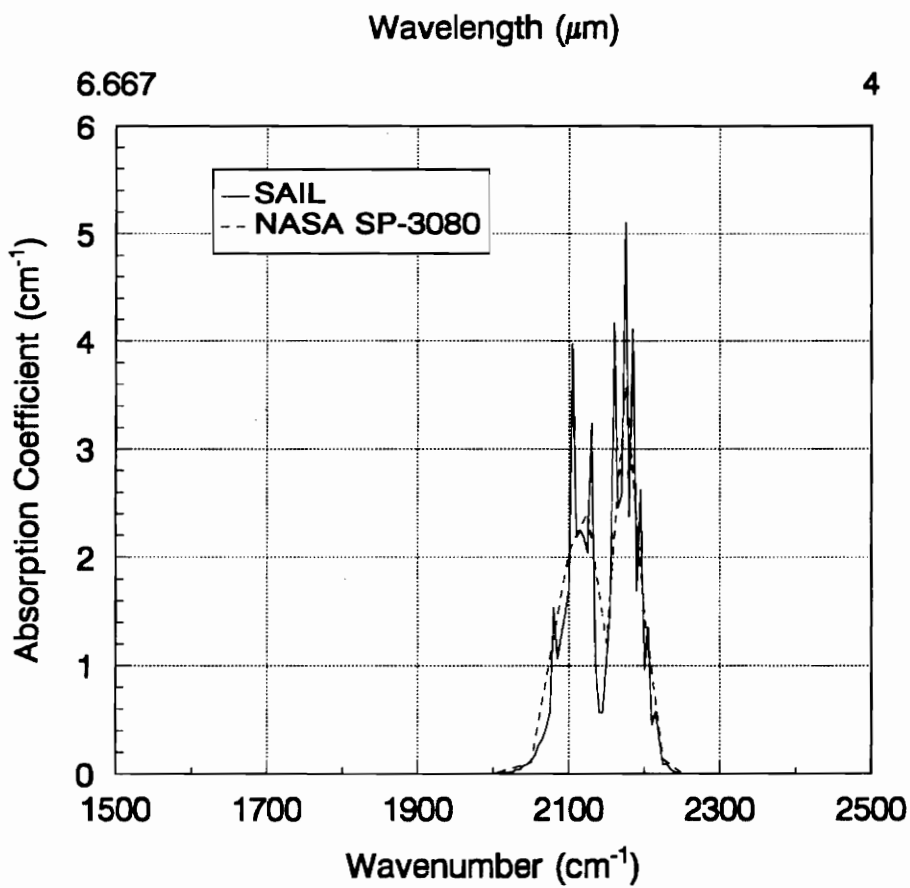


Figure 19. Comparison of the band-averaged absorption coefficient provided by NASA SP-3080 and Program SAIL for carbon monoxide at 300 K.

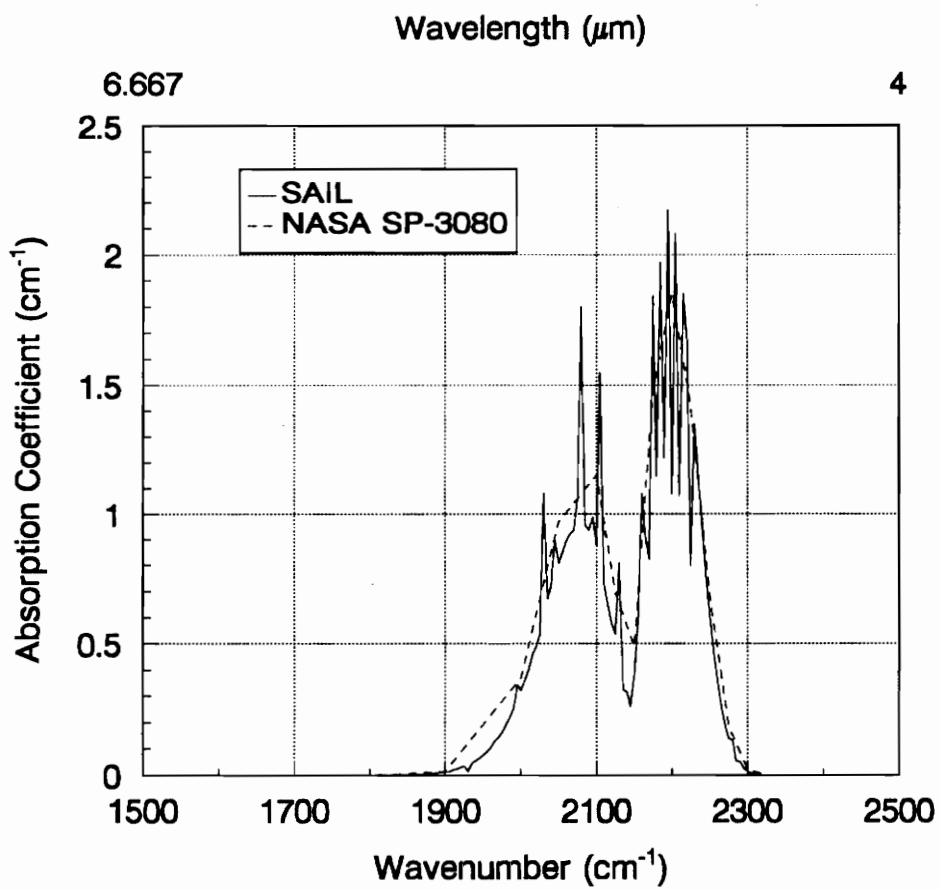


Figure 20. Comparison of the band-averaged absorption coefficient provided by NASA SP-3080 and Program SAIL for carbon monoxide at 1200 K.

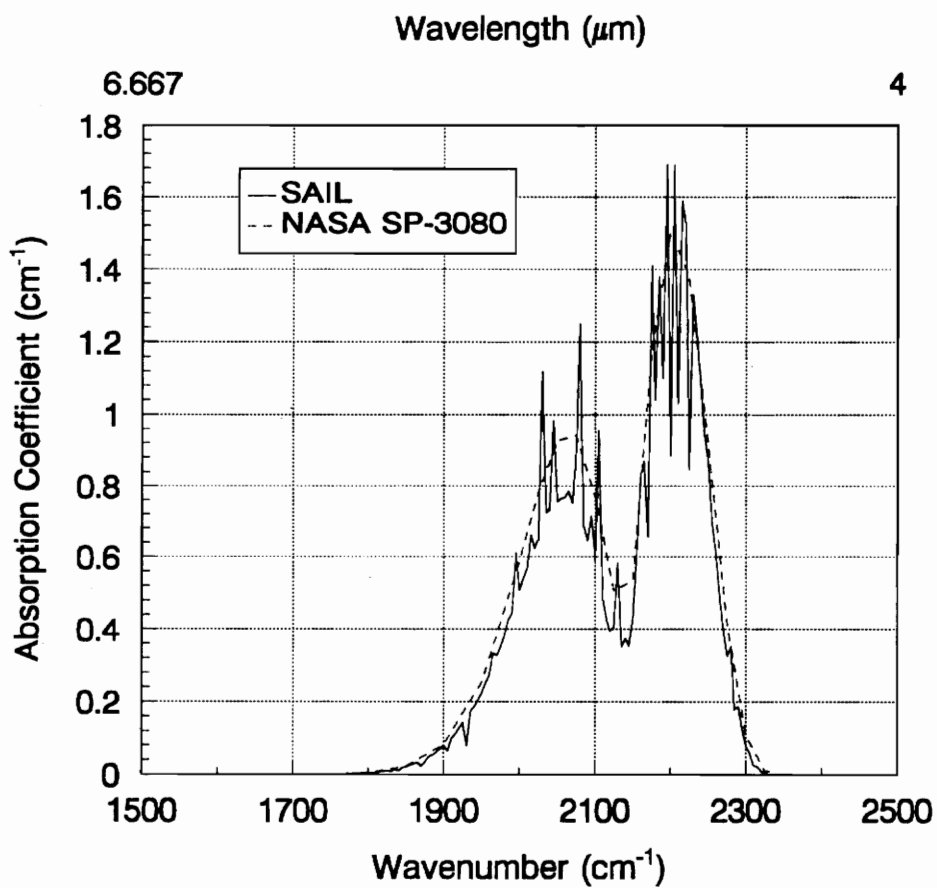


Figure 21. Comparison of the band-averaged absorption coefficient provided by NASA SP-3080 and Program SAIL for carbon monoxide at 1800 K.

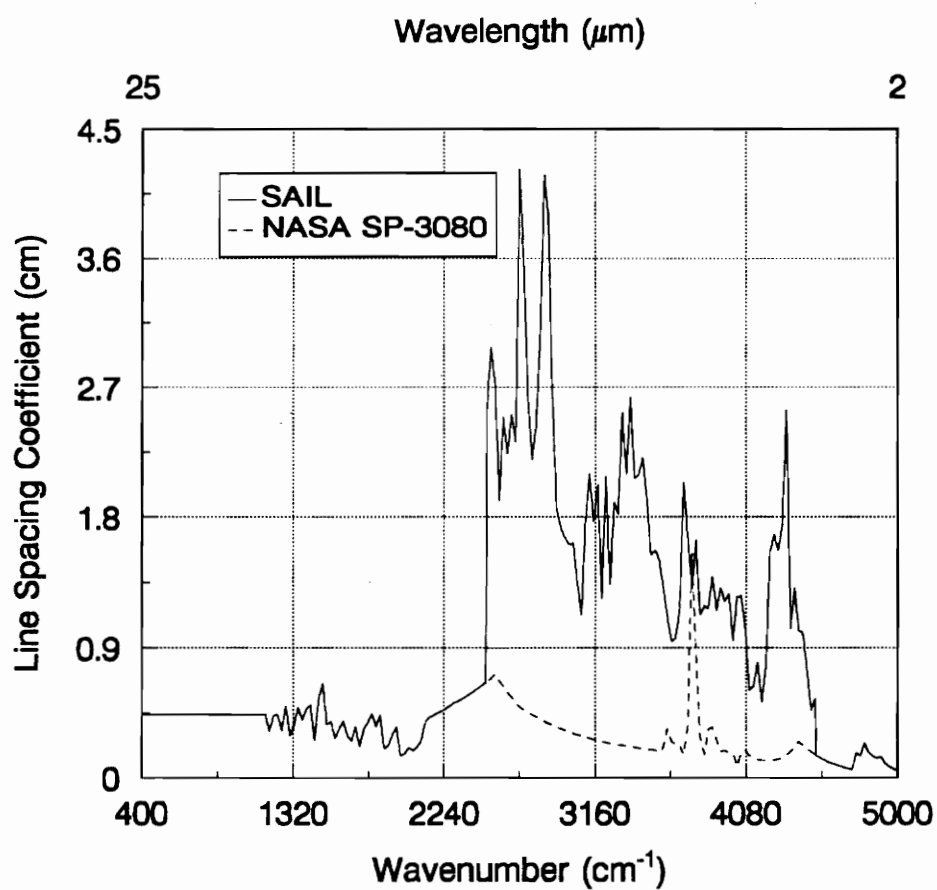


Figure 22. Comparison of the line spacing coefficient provided by NASA SP-3080 and Program SAIL for water vapor at 600 K.

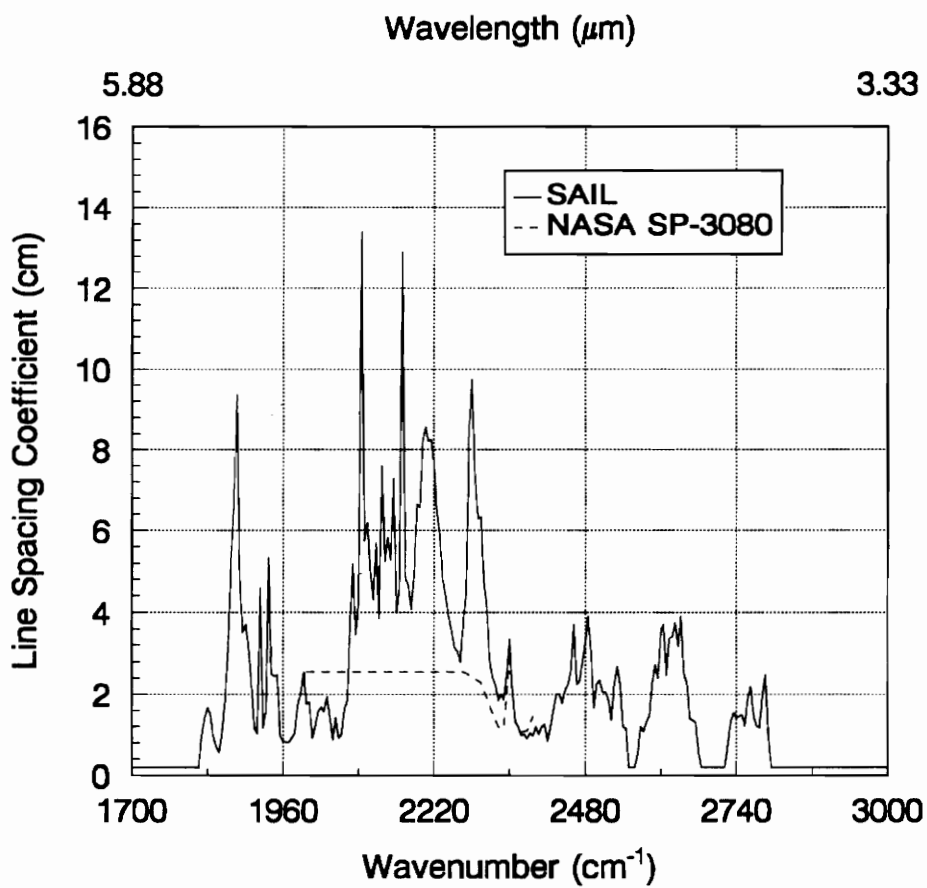


Figure 23. Comparison of the line spacing coefficient provided by NASA SP-3080 and Program SAIL for carbon dioxide at 300 K.

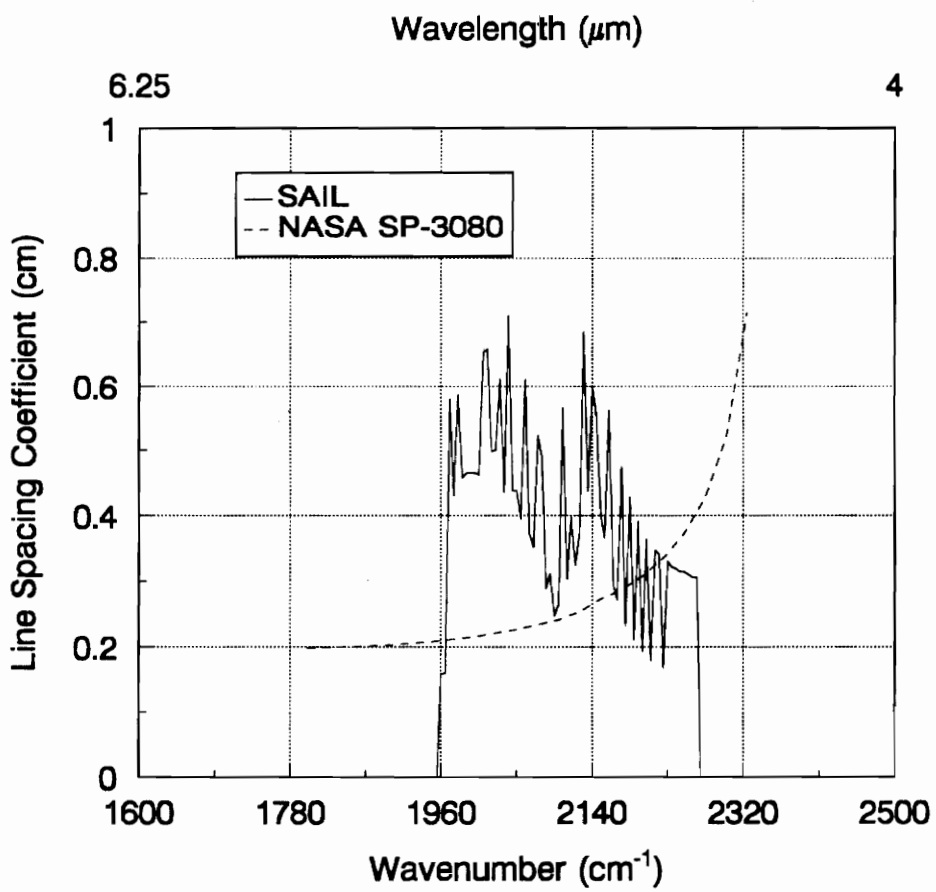


Figure 24. Comparison of the line spacing coefficient provided by NASA SP-3080 and Program SAIL for carbon monoxide at 300 K.

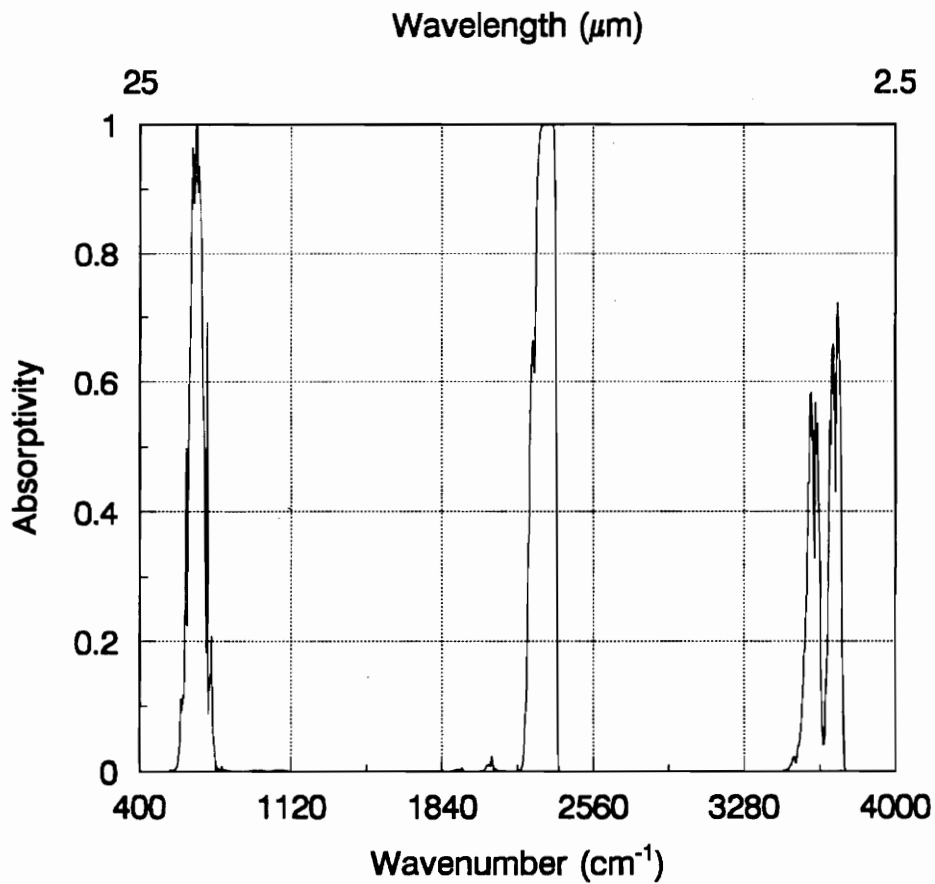


Figure 25. Absorptivity of dry air: an example of the usefulness of the low temperature data provided by SAIL. SAIL input parameters: Temperature = 285 K, Pressure = 1 atm, Path Length = 100 m, Percent by Volume; Nitrogen = 78.084, Oxygen = 20.948, Carbon Dioxide = 0.0314.

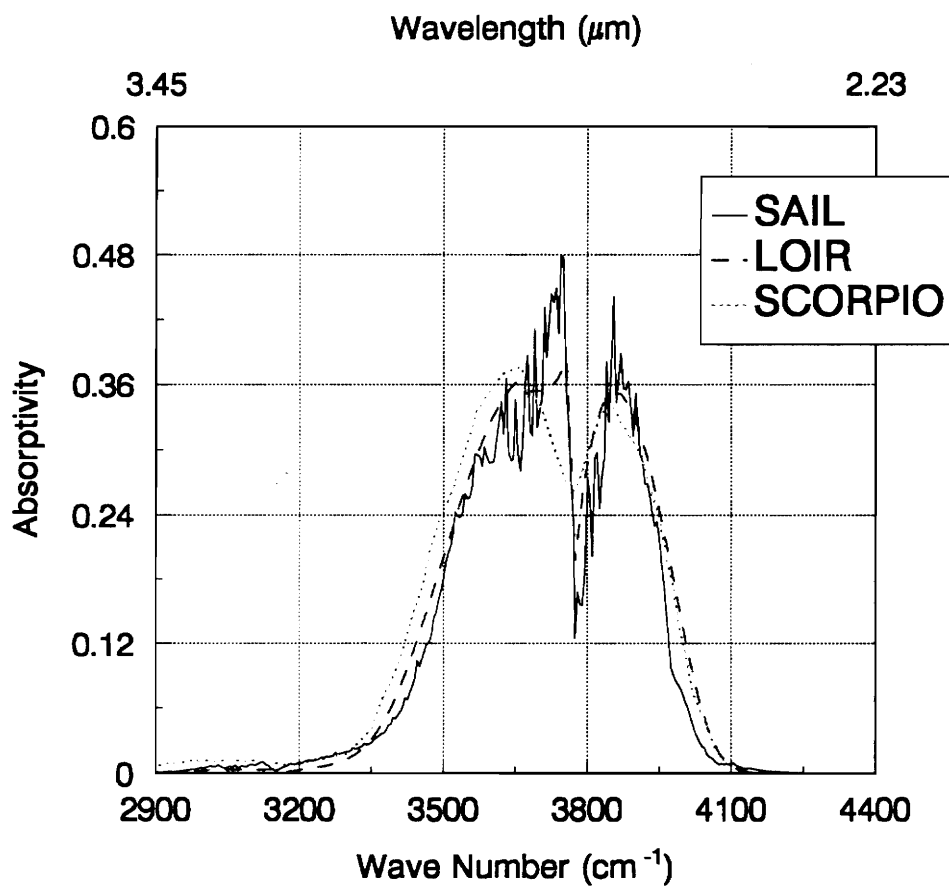


Figure 26. Comparison of results obtained using SAIL, LOIR, and SCORPIO for Heated Water Vapor at Low Pressures. Temperature = 555.5 K, Pressure = 0.11 atm, Path Length = 23.47 cm.

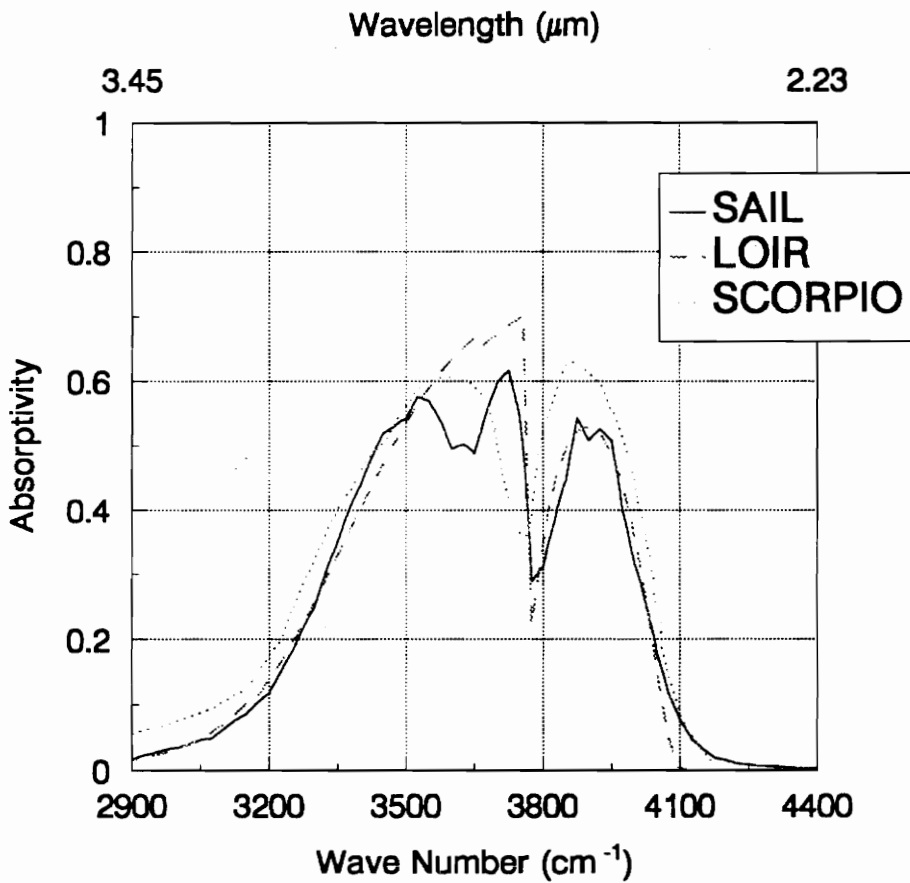


Figure 27. Comparison of results obtained using SAIL, LOIR, and SCORPIO for heated water vapor. Temperature = 1111.1 K, Pressure = 0.6 atm, Path Length = 23.47 cm.

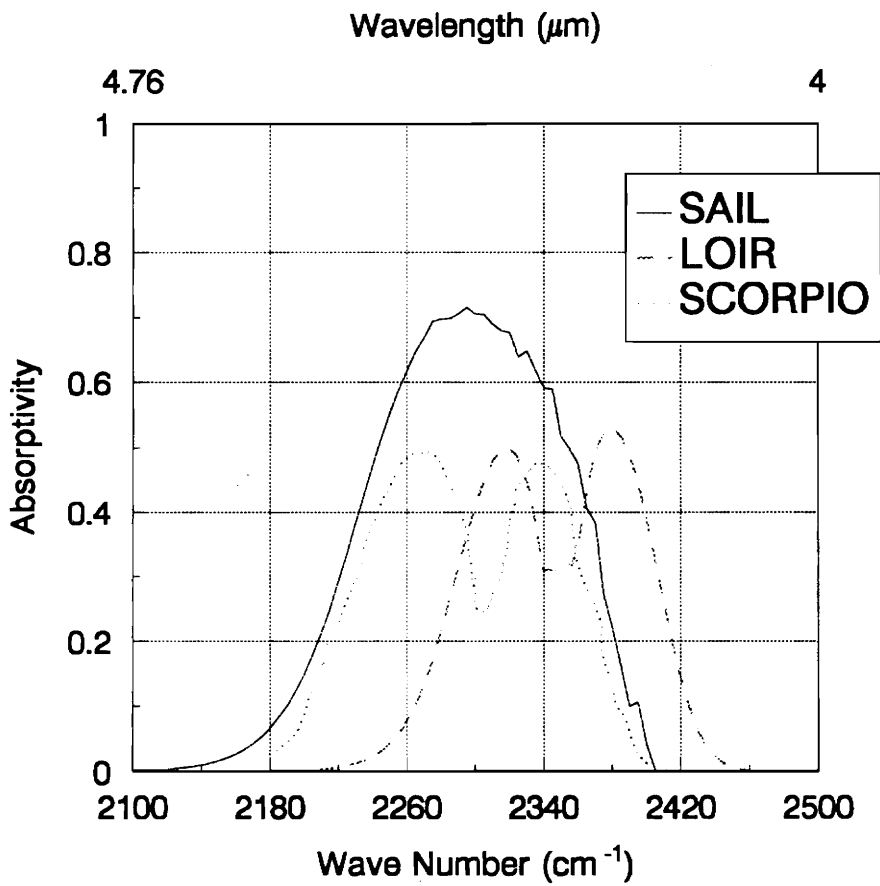


Figure 28. Comparisons of results obtained using SAIL, LOIR, SCORPIO for heated carbon dioxide at low pressures. Temperature = 1199.67 K, Pressure = 0.06 atm, Path Length = 7.75 cm.

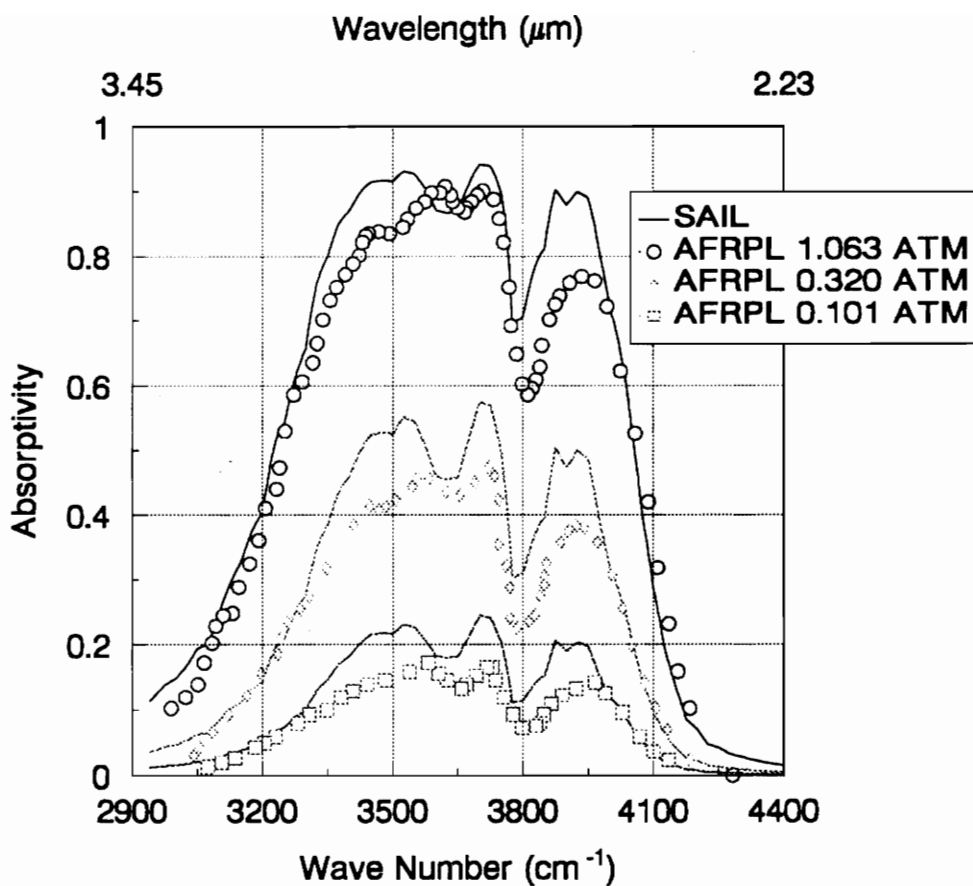


Figure 29. Comparison of SAIL with AFRPL experimental data for isothermal hot water vapor at various pressures. Temperature = 1177 K, Path Length = 60 cm. Volume by Percent: Water Vapor = 100 [23].

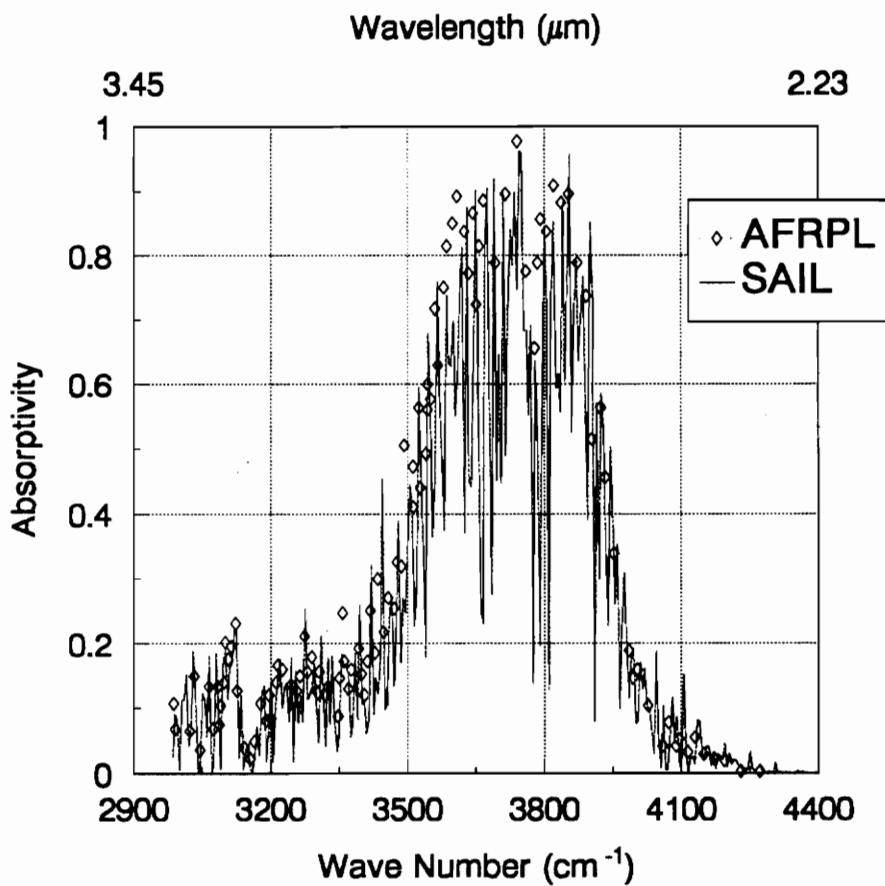


Figure 30. Comparison of SAIL with AFRPL experimental data for isothermal cold water vapor. Temperature = 296 K, Pressure = 0.07 atm, Path Length = 10,000 cm. Volume by Percent: Water Vapor = 0.143, Nitrogen = 0.857 [23].

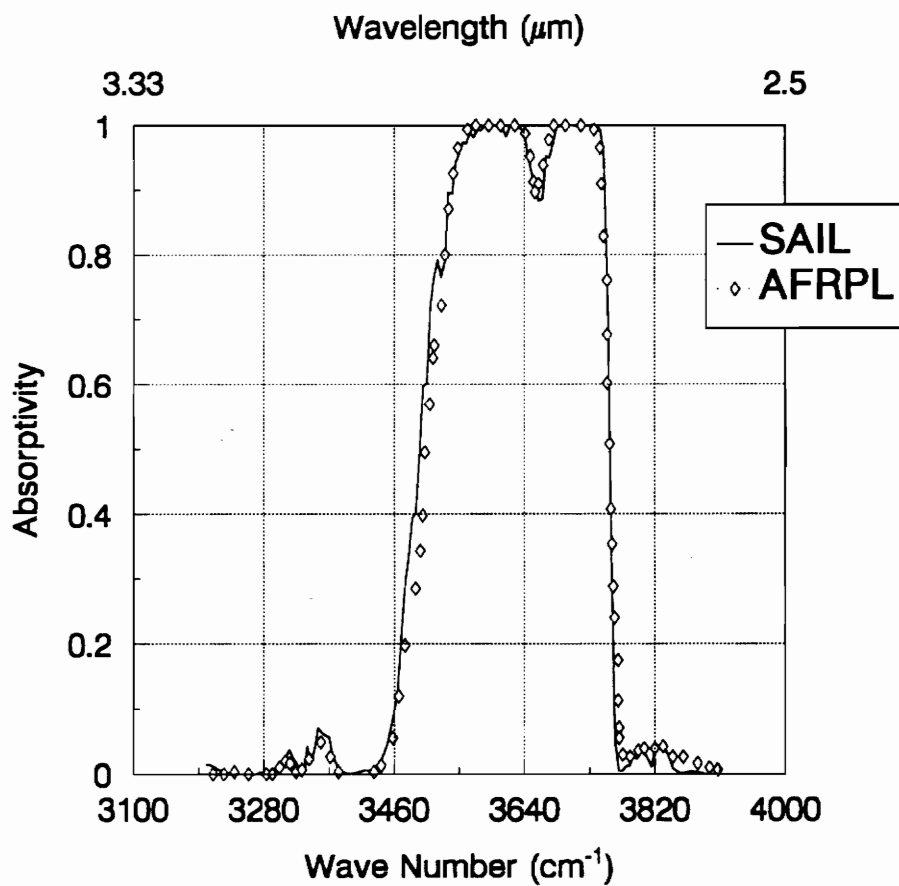


Figure 31. Comparison of SAIL with AFRPL experimental data for isothermal cold carbon dioxide. Temperature = 295 K, Pressure = 0.129 atm, Path Length = 10,000 cm. Volume by Percent: Carbon Dioxide = 0.904, Nitrogen = 0.096 [23].

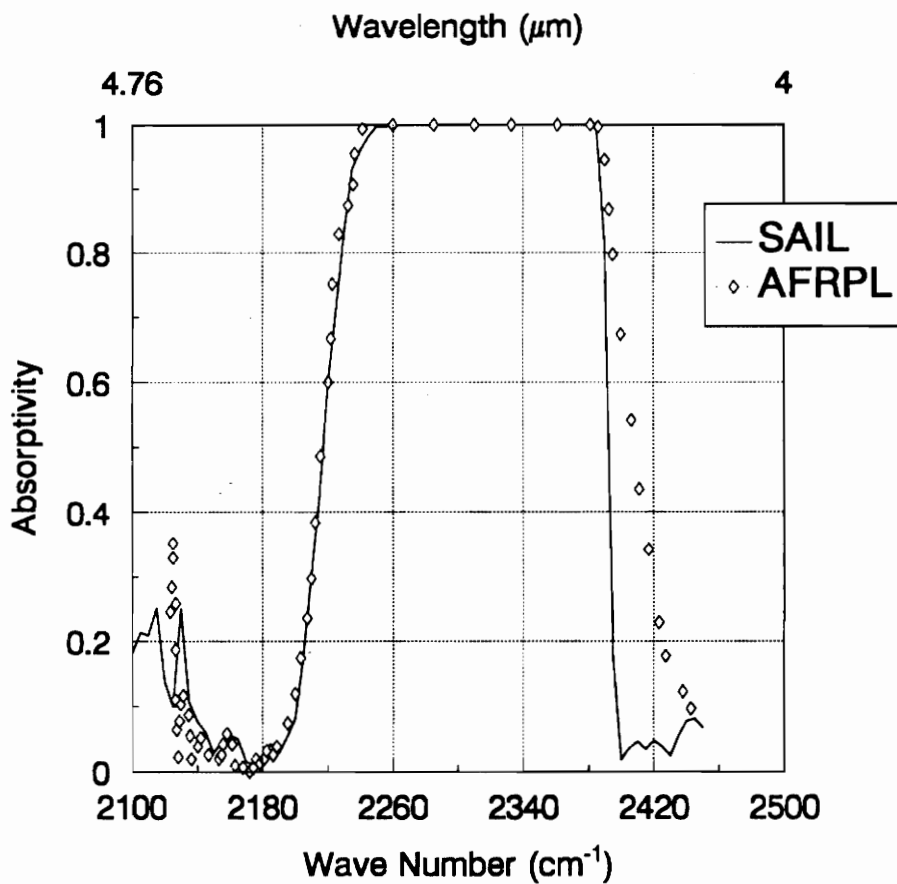


Figure 32. Comparison of SAIL with AFRPL experimental data for an isothermal cold mixture. Temperature = 297 K, Pressure = 0.129 atm, Path Length = 10,000 cm. Volume by Percent: Water Vapor = 0.088, Carbon Dioxide = 0.904, Nitrogen = 0.007 [23].

Tables

Table 1. Model values for the collision line width parameters.

Molecule (n)	Broadener (m)	$(\gamma_{n,m})_{273}$ $\text{cm}^{-1}\text{atm}^{-1}$	$\eta_{n,m}$	$(\gamma_{n,n})_{273}$ $\text{cm}^{-1}\text{atm}^{-1}$	$\eta_{n,n}$
H ₂ O	H ₂ O	(0.09)	0.5	0.44	1.0
	N ₂	0.09	0.5		
	O ₂	0.04	0.5		
	H ₂	(0.05)	0.5		
	CO ₂	0.12	0.5		
	CO	(0.10)	0.5		
CO ₂	CO ₂	0.09	0.5	0.01	1.0
	H ₂ O	(0.07)	0.5		
	N ₂	0.07	0.5		
	O ₂	0.055	0.5		
	H ₂	0.08	0.5		
	CO	(0.06)	0.5		
CO	CO	0.06	0.5	0.0	1.0
	H ₂ O	(0.06)	0.5		
	CO ₂	(0.07)	0.5		
	H ₂	0.06	0.5		
	N ₂	0.06	0.5		
	O ₂	0.05	0.5		

Note: Table 1 shows model values for only H₂O, CO₂, and CO. Other model values are available for NO, CN, OH, HCl, and HF [20]. Values in parenthesis are estimated.

Table 2. Example of the carbon dioxide band-averaged absorption coefficients.

Wavenumber (cm ⁻¹)	100 K	300 K	1200 K
2000	0.742E-08	0.714E-05	0.873E-05
2005	0.813E-07	0.119E-04	0.144E-04
2010	0.620E-06	0.162E-04	0.211E-04
2015	0.317E-05	0.219E-04	0.309E-04
2020	0.101E-04	0.283E-04	0.448E-04
2025	0.192E-04	0.384E-04	0.650E-04
2030	0.244E-04	0.120E-03	0.937E-04
2035	0.573E-04	0.295E-03	0.134E-03
2040	0.110E-04	0.632E-03	0.192E-03
2045	0.118E-04	0.123E-02	0.273E-03
2050	0.114E-03	0.302E-02	0.386E-03
2055	0.493E-03	0.324E-02	0.545E-03
2060	0.160E-02	0.335E-02	0.765E-03
2065	0.313E-02	0.316E-02	0.107E-02
2070	0.406E-02	0.213E-02	0.149E-02
2075	0.106E-01	0.742E-02	0.206E-02

Note: The band-averaged absorption coefficient is compiled for the gases, H₂O, CO₂, and CO for use in SAIL. The coefficients are listed from 400 to 5000 wavenumbers in 5 wavenumber increments. Values are listed at several temperatures, 100 K, 200 K, 300 K, 600 K, 1200 K, 1800 K, 2400 K, 3000 K [18].

Table 3. Example of the carbon dioxide line spacing coefficients.

Wavenumber (cm ⁻¹)	100 K	300 K	1200 K
2000	0.118E+01	0.176E+01	0.266E+03
2005	0.111E+01	0.180E+01	0.322E+03
2010	0.583E+00	0.914E+00	0.332E+03
2015	0.609E+00	0.120E+01	0.348E+03
2020	0.659E+00	0.158E+01	0.358E+03
2025	0.768E+00	0.168E+01	0.370E+03
2030	0.123E+01	0.157E+01	0.380E+03
2035	0.334E+01	0.194E+01	0.390E+03
2040	0.373E+01	0.147E+01	0.402E+03
2045	0.287E+01	0.878E+00	0.410E+03
2050	0.293E+01	0.143E+01	0.418E+03
2055	0.746E+00	0.922E+00	0.428E+03
2060	0.667E+00	0.102E+01	0.434E+03
2065	0.712E+00	0.164E+01	0.442E+03
2070	0.864E+00	0.184E+01	0.446E+03
2075	0.259E+01	0.386E+01	0.450E+03

Note: The line spacing coefficient is compiled for the gases, H₂O, CO₂, and CO for use in SAIL. The coefficients are listed from 400 to 5000 wavenumbers in 5 wavenumber increments. Values are listed at several temperatures, 100 K, 200 K, 300 K, 600 K, 1200 K, 1800 K, 2400 K, 3000 K [18].

References

1. Hardman, R.R., Smith, M.H., Gelhausen, P.A., Van Dalsem, W.R., Mahan, J.R., *Infrared Imaging: A Validation Technique for Computational Fluid Dynamics Codes Used in STOVL Applications*, AIAA Paper 91-0675, 29th Aerospace Sciences Meeting, Reno, Nevada, January 7-10, 1991.
2. Hardman, R.R. **Infrared Imaging: A Proposed Validation Technique for Computational Fluid Dynamics Codes Used in STOVL Applications**, M.S. Thesis, Virginia Polytechnic Institute and State University, Blacksburg, VA, May 1990.
3. Milford, C.M., *Hot Gas Recirculation in V/STOL*, SAE Paper 872036, International Powered Lift Conference and Exposition, Santa Clara, California, December 7-10, 1987.
4. Stewart, V.R., Kuhn, R.E., *A method for Estimating the Propulsion Induced Aerodynamic Characteristics of STOL Aircraft in Ground Effect*, NADC-80226-60, August 1983.

5. Kuhn, R.E., *Hover Suckdown and Fountain Effects*, SAE Paper 872305, International Powered Lift Conference and Exposition, Santa Clara, California, December 7-10, 1987.
6. Van Dalsem, W.R., Panaras, A.G., Steger, J.L., *Numerical Investigation of a Jet in Ground Effect with a Crossflow*, SAE paper 872344, International Powered-Lift Conference and Exposition, Santa Clara, California, December 7-10, 1987.
7. Chawla, K., Van Dalsem, W.R., Rao, K.V., *Numerical Study of a Delta Planform with Multiple Jets in Ground Effect*, SAE paper 892283, SAE Aerospace Technology Conference, Anaheim, California, September 25-28, 1989.
8. Smith, M.H., Van Dalsem, W.R., Chawla, K., Dougherty, F.C., *Numerical Simulation of a Complete STOVL Aircraft in Ground Effect*, AIAA 9th Applied Aerodynamics Conference, Baltimore, Maryland, September 23-25, 1991.
9. Birckelbaw, L., Nelson, E.L., *Infrared Flow Visualization of V/STOL Aircraft*, AIAA paper to be presented at the Aircraft Design Systems Meeting, Hilton Head, South Carolina, August 24-26, 1992.
10. Anon., **User's Manual to Version 4.2.1**, Agema Infrared Systems, Danderyd, Sweden, December, 1991.
11. Anon., **Burst Recording Unit, Introduction Manual, Reference Manual**,

- Version 3.1**, Agema Infrared Systems, Danderyd, Sweden, September, 1990.
12. Vanderbilt, D., Slack, M., *A Model for Emission and Scattering of Infrared Radiation from Combustion Gases and Particles*, Grumman Research Department Memorandum, RM-621, June 1976.
 13. Kim, S.J., Caldwell, J., *Real Line Strength Distributions for Random Band Models*, **Journal Quantitative Spectroscopy and Radiant Transfer**, Vol. 29, No. 2, 1983, pp. 151-156.
 14. Pierluissi, J. H., Maragaoudakis, C.E., *Molecular Transmittance Band Model for Oxygen in the Infrared*, **Applied Optics**, Vol. 25, No. 10, 1986, pp 1538-1540.
 15. Drakes, J., Hiers, R., Reed, R., *Doppler Shift Effects on Infrared Band Model Calculations*, AIAA Paper 89-1678, 24th Thermophysics Conference, Buffalo, New York, June 12-14, 1989.
 16. Felske, J.D., Tien, C.L., *Wide Band Characterization of the Total Band Absorptance of Overlapping Infrared Gas Bands*, **Combustion Science and Technology**, Vol 11, 1975, pp. 111-117.
 17. Kneizys, F.X., Anderson, G.P., Shettle, E.P., Gallery, W.O., Abreu, L.W., Selby, J.E.A., Chetwynd, J.H., Clough, S.A., **Users Guide to LOWTRAN 7**, Air Force Geophysics Laboratory Paper, AFGL-TR-88-0177, August 1988.

18. Baars, J., **NIRATAM Users Manual, Version 2.1**, SHAPE Technical Centre, The Hague, The Netherlands, July 23, 1991.
19. Mahan, J.R., Stern, C.H., Nelson, E.L., Turk, J., Villeneuve, P.V., **LOIR Programmers' Manual, General Electric Aircraft Engines, Aircraft Survivability Technology**. The Mechanical Engineering Department, Virginia Polytechnic Institute & State University, Blacksburg, VA, Prepared under NASA Ames Grant NAG 2-664, October, 1991.
20. Ludwig, C.B., Malkmus, W., Reardon, J.E., Thomson, J.A.L., **Handbook of Infrared Radiation from Combustion Gases**, Prepared by: Marshall Space Flight Center, National Aeronautics and Space Administration Special Publication, NASA SP-3080, 1973
21. Siegel, L.R., Howell, J.R., **Thermal Radiation Heat Transfer**, Second Edition, McGraw Hill, New York, 1972.
22. Goody, R.M., Yung, Y.L., **Atmospheric Radiation, Theoretical Basis**, Second Edition, Oxford University Press, New York, 1989.
23. Sukanek, P.C., Davis, L.P., *An Assessment of the NASA Band Model Formulation for Calculating the Radiance and Transmission of Hot and Cool Gases*, Air Force Rocket Propulsion Laboratory Paper, AFRPL-TR-76-9, February, 1976
24. Cummings, M., General Electric Aircraft Engines, *Personal Communication*, September 1990.

25. Cornet, B., Photon Research Associates, *Personal Communication*, May 1990.
26. Agema Infrared Systems, Sales Brochure of Agema Thermovision® Dual 880 Infrared Imaging System, Danderyd, Sweden, 1990.
27. Birckelbaw, L., National Aeronautics and Space Administration Ames Research Center, *Personal Communication*, July 1990.

Appendix A SAIL Sample Execution

Appendix A SAIL Sample Execution

The following is a sample execution of Program SAIL as it would appear to the program user. This execution is from a VAX workstation. User answers are in **bold type**.

VAX>**R SAIL**

READING IN ABSORPTION COEFFICIENTS AND FINE
STRUCTURE PARAMETERS.....

Enter [1] wavelength (micrometer)
 [2] wave number (cm**⁻¹)

1

Please Enter the wavelength range ...

NOTE: No less than 2 microns

NOTE: No greater than 25 microns

2.5,2.7

CONVERTING WV1 AND WV2....

WV1.... 3703.704

WV2.... 4000.000

Please input the Temperature [K]....

650.

Please input the total pressure [ATM]....

2.2

These Molecular Constituents are CURRENTLY available
in any combination:

- [1] H2O Water Vapor
- [2] CO2 Carbon Dioxide
- [3] CO Carbon Monoxide
- [4] NO Nitrogen Oxide
- [5] CN
- [6] OH
- [7] HCl

[8] HF
[9] N2 Nitrogen
[10] O2 Oxygen
[11] H2 Hydrogen

Only Constituents [1],[2],[3] will absorb or emit radiation. Constituents [4] through [11] will act to broaden the effects of [1],[2], and [3].

Description of the Gas.....

PLEASE Enter mole fraction of [1] H2O Water Vapor
0.2

PLEASE Enter mole fraction of [2] CO2 Carbon Dioxide
0.5

PLEASE Enter mole fraction of [3] CO Carbon Monoxide
0.1

PLEASE Enter mole fraction of [4] NO Nitrogen Oxide
0

PLEASE Enter mole fraction of [5] CN
0

PLEASE Enter mole fraction of [6] OH
0

PLEASE Enter mole fraction of [7] HCl
0

PLEASE Enter mole fraction of [8] HF
0

PLEASE Enter mole fraction of [9] N2 Nitrogen
0.1

PLEASE Enter mole fraction of [10] O2 Oxygen
0.1

PLEASE Enter mole fraction of [11] Hydrogen
0

Please Enter the Path Length [CM].....'
15

```
Please Enter the output data filename...'  
SAMPLE.DAT
```

```
Do you want a file header ? [y/n]'  
Y
```

```
RUN PROGRAM AGAIN ? (Y/N) '  
N
```

```
FORTRAN STOP
```

The output file corresponding to this execution is shown in Appendix B,
SAIL Sample Results.

Appendix B SAIL Sample Results

Appendix B Sail Sample Results

The following is a Program SAIL output file. It is presented in conjunction with Appendix A, SAIL Sample execution.

PROGRAM SAIL OUTPUT

```
TEMPERATURE           =      650.00
TOTAL PRESSURE        =         2.20
PATH LENGTH (cm)     =         15.00
STARTING WAVENUMBER  =      3700.00
ENDING WAVENUMBER    =      4000.00
```

MOLE FRACTIONS OF CONSTITUENTS:

```
H2O .. 0.200000    CO2... 0.500000
CO.... 0.100000    NO.... 0.000000
CN.... 0.000000    OH.... 0.000000
HCl... 0.000000    HF.... 0.000000
N2.... 0.100000    O2.... 0.100000
H2.... 0.000000
```

WAVENUMBER	ABSORPTIVITY	TRANSMITTANCE
3700.000	0.9848202	1.5179782E-02
3705.000	0.9871430	1.2857047E-02
3710.000	0.9750146	2.4985377E-02
3715.000	0.9421589	5.7841126E-02
3720.000	0.9717271	2.8272841E-02
3725.000	0.9883233	1.1676653E-02
3730.000	0.9936740	6.3259499E-03
3735.000	0.9945768	5.4231770E-03
3740.000	0.9940669	5.9330901E-03
3745.000	0.9806113	1.9388685E-02
3750.000	0.9554074	4.4592623E-02
3755.000	0.8788440	0.1211561
3760.000	0.7462723	0.2537278
3765.000	0.5856998	0.4143002
3770.000	0.4300780	0.5699220
3775.000	0.2828779	0.7171221

3780.000	0.3030918	0.6969082
3785.000	0.3216227	0.6783773
3790.000	0.3397787	0.6602213
3795.000	0.3549311	0.6450689

<etc...>

3895.000	0.6035340	0.3964660
3900.000	0.5923080	0.4076920
3905.000	0.5814647	0.4185353
3910.000	0.5696791	0.4303209
3915.000	0.5568800	0.4431200
3920.000	0.5430986	0.4569014
3925.000	0.5287110	0.4712891
3930.000	0.5155764	0.4844236
3935.000	0.5024338	0.4975663
3940.000	0.4891129	0.5108871
3945.000	0.4744882	0.5255118
3950.000	0.4602020	0.5397980
3955.000	0.4260496	0.5739504
3960.000	0.3878329	0.6121671
3965.000	0.3448232	0.6551768
3970.000	0.2972220	0.7027780
3975.000	0.2415819	0.7584181
3980.000	0.2313189	0.7686811
3985.000	0.2204712	0.7795288
3990.000	0.2096025	0.7903975
3995.000	0.1984486	0.8015514
4000.000	0.1873710	0.8126290

Appendix C SAIL Source Code Listing

```

PROGRAM SAIL
C*****
C*****
C   PROGRAM:      SAIL.FOR
C   WRITTEN BY:   EDWARD L. NELSON
C   ADVISOR:      J. R. MAHAN, PHD
C                 VIRGINIA POLYTECHNIC INSTITUTE AND STATE UNIVERSITY
C                 DEPARTMENT OF MECHANICAL ENGINEERING
C                 BLACKSBURG, VA  24061
C
C   UNDER CONTRACT NUMBER:
C                 NCC 2-691 AT THE
C                 NASA AMES RESEARCH CENTER
C                 MOFFETT FIELD, CA
C
C   SAIL ( SELECTIVE ANALYTIC INFRARED LOGIC ) IS AN INFRARED
C   BAND MODEL ADAPTED FROM NASA SP-3080.
C
C-----LIST OF ARRAYS IN SAIL.FOR-----
C A1(999,15)..BAND-AVERAGED ABSORPTION COEFFICIENTS FOR WATER VAPOR
C A2(999,15)..BAND-AVERAGED ABSORPTION COEFFICIENTS FOR CARBON DIOXIDE
C A3(999,15)..BAND-AVERAGED ABSORPTION COEFFICIENTS FOR CARBON MONOXIDE
C A1L(999,15)..LINE SPACING PARAMETERS FOR WATER VAPOR
C A2L(999,15)..LINE SPACING PARAMETERS FOR CARBON DIOXIDE
C A3L(999,15)..LINE SPACING PARAMETERS FOR CARBON MONOXIDE
C PP(15)..PARTIAL PRESSURES OF THOSE GASES
C DELU(15)..STP ADJUSTED PATH LENGTH FOR EACH SPECIES
C GAMC(15)..COLLISION BROADENED HALF WIDTH FOR EACH SPECIES
C GAMD(15,999)..DOPPLER BROADENED HALF WIDTH FOR EACH WAVENUMBER
C AKAP(15,999)..TEMPERATURE CORRECTED BAND-AVERAGED ABSORPTION
C   COEFFICIENT FOR EACH SPECIES
C SPAC(15,999)..TEMPERATURE CORRECTED LINE SPACING PARAMETER FOR
C   EACH SPECIES
C ASUBC(15,999)..COLLISION BROADENED FINE STRUCTURE PARAMETER
C ASUBD(15,999)..DOPPLER BROADENED FINE STRUCTURE PARAMETER
C XSUBC(15,999)..OPTICAL DEPTH FOR A PURE COLLISION CURVE OF GROWTH
C XSUBD(15,999)..OPTICAL DEPTH FOR A PURE DOPPLER CURVE OF GROWTH
C YSUBN(15,999)..COMBINED COLLISION AND DOPPLER OPTICAL DEPTHS
C XSTAR(15,999)..OPTICAL DEPTH FOR THE WEAK LINE LIMIT
C XSUBN(15,999)..OPTICAL DEPTH
C X(999)..OPTICAL DEPTH OF MIXTURE, STORED BY WAVENUMBER
C ABS(999)..FRACTION OF RADIANT ENERGY ABSORBED BY VOLUME ELEMENT
C TRANS(999)..TRANSMITTANCE OF VOLUME ELEMENT
C
C-----LIST OF VARIABLES IN SAIL.FOR-----
C DELX..PATH LENGTH (cm)
C WV1..BEGINNING WAVENUMBER (1/cm)
C WV2..ENDING WAVENUMBER (1/cm)
C NDIV..NUMBER OF DIVISIONS IN THE WAVENUMBER RANGE (-)
C T..AVERAGE TEMPERATURE OF THE PATH LENGTH (K)
C P..AVERAGE TOTAL PRESSURE OF THE PATH LENGTH (ATM)
C WV..CURRENT WAVENUMBER (1/cm)
C X..OPTICAL DEPTH (-)
C FNAME1..USER SPECIFIED-OUTPUT DATA FILENAME
C AGAIN--(Y OR N) USED TO TELL IF USER WANTS TO RUN PROGRAM AGAIN
C
C DIMENSION STATEMENTS AND COMMON BLOCKS
C   COMMON/ THICK/ DELX,DELU(15)
C   COMMON/ WAVE/ WV1,WV2,INT,NDIV
C   COMMON/ STUFF/ T,P,PP(20),WV,FNAME1
C   COMMON/ NIRDATA/ A1(999,12),A1L(999,12),A2(999,12),
C   $           A2L(999,12),A3(999,12),A3L(999,12)
C   COMMON/ GAMMA/ GAMC(20),GAMD(12,999)
C   COMMON/ SPACE/ AKAP(12,999),SPAC(12,999)

```

```

COMMON/ STARDM/ XSTAR(12,999)
COMMON/ FINEST/ ASUBD(12,999),ASUBC(12,999)
COMMON/ DEPTH/ XSUBD(12,999),XSUBC(12,999)
COMMON/ OPTIC/ YSUBN(12,999),XSUBN(12,999),X(999)
COMMON/ MOLES/ AMOL(20)
COMMON/ RESULT/ ABS(999),TRANS(999)

CHARACTER AGAIN*5,FNAM1*20

C ROUTINE TO READ IN NIRATAM ABSORPTION AND LINE SPACING COEFFICIENTS
  CALL NIRATDAT

C ROUTINE FOR USER INPUT PROGRAM PARAMETERS
  1 CALL EXPRESS

C ROUTINE TO COMPUTE THE ABSORPTION AND LINE SPACING COEFFICIENTS
C FOR THE APPROPRIATE TEMPERATURE AND WAVELENGTH RANGE
  CALL SKATEPRO

C ROUTINE TO COMPUTE STP ADJUSTED PATH LENGTH
  CALL DELTAU

C COMPUTE THE DOPPLER AND COLLISION BROADENED HALF WIDTHS
  CALL BROADEN

C ROUTINE TO COMPUTE OPTICAL DEPTH FOR THE WEAK LINE LIMIT
  CALL STAR

C ROUTINE TO COMPUTE THE COLLISION AND DOPPLER BROADENED FINE
C STRUCTURE PARAMETER
  CALL FINER

C ROUTINE TO COMPUTE THE OPTICAL DEPTH FOR A PURE DOPPLER CURVE
C OF GROWTH AND A PURE COLLISION CURVE OF GROWTH
  CALL GROWTH

C ROUTINE TO COMPUTE THE COMBINED COLLISION AND DOPPLER OPTICAL
C DEPTHS
  CALL OPCLOD

C WRITE DATA TO A FILE
  CALL WRITER

C RUN AGAIN OPTION
  WRITE(*,*)' RUN PROGRAM AGAIN ? (Y/N) '
  READ(*,'(A5)') AGAIN
  IF( (AGAIN .EQ. 'Y') .OR. (AGAIN .EQ. 'y') ) THEN
    GOTO 1
  ENDIF

C STOP COMPILATION AND END THE PROGRAM
  STOP
  END
C-----

```

```

SUBROUTINE NIRATDAT
C*****
C*****
C THIS ROUTINE READS IN THE NIRATAM ABSORPTION COEFFICIENTS AND LINE
C SPACING COEFFICEINTS FROM A FILE AND STORES THEIR VALUES IN
C DIFFERENT ARRAYS.
C
C-----LIST OF VARIABLES IN NIRATDAT-----
C----- (NOT MENTIONED PREVIOUSLY) -----
C FNAME..CHARACHTER VARIABLE, NIRATAM DATA FILENAME
C I..INTEGER INDEXING VARIABLE
C J..INTEGER INDEXING VARIABLE
C
C DIMENSION STATEMENTS AND COMMON BLOCKS
COMMON/ NIRDATA/ A1(999,12),A1L(999,12),A2(999,12),
$      A2L(999,12),A3(999,12),A3L(999,12)

CHARACTER*20 FNAME

C OPEN THE DATA FILE
FNAME = 'MOLPLUME.DAT'

OPEN(UNIT = 13, FILE = FNAME, STATUS='UNKNOWN')

C CLEAR THE SCREEN
DO 3 J=1,27
3 WRITE(*,*)

C MESSAGE TO THE PROGRAM USER
WRITE(*,*)
WRITE(*,*) ' READING IN ABSORPTION COEFFICIENTS AND FINE'
WRITE(*,*) ' STRUCTURE PARAMETERS.....'

C READ IN WATER VAPOR ABSORPTION COEFFICIENTS

READ(13,4)
4 FORMAT(////)

DO 100 I=1,921
READ(13,5) WV,A1(I,1),A1(I,2),A1(I,3),A1(I,4),A1(I,5),
$      A1(I,6),A1(I,7),A1(I,8)
5 FORMAT(1X,F6.1,1X,8(E9.3))
100 CONTINUE

C READ IN WATER VAPOR LINE SPACING COEFFICIENTS

READ(13,4)
DO 200 I=1,921
READ(13,5) WV,A1L(I,1),A1L(I,2),A1L(I,3),A1L(I,4),A1L(I,5),
$      A1L(I,6),A1L(I,7),A1L(I,8)
200 CONTINUE

C READ IN CARBON DIOXIDE ABSORPTION COEFFICIENTS

READ(13,4)
DO 300 I=1,921
READ(13,5) WV,A2(I,1),A2(I,2),A2(I,3),A2(I,4),A2(I,5),
$      A2(I,6),A2(I,7),A2(I,8)
300 CONTINUE

C READ IN CARBON DIOXIDE LINE SPACING COEFFICIENTS

READ(13,4)
DO 400 I=1,921
READ(13,5) WV,A2L(I,1),A2L(I,2),A2L(I,3),A2L(I,4),A2L(I,5),

```

```

$          A2L(I,6),A2L(I,7),A2L(I,8)
400 CONTINUE

C READ IN CARBON MONOXIDE ABSORPTION COEFFICIENTS

  READ(13,4)
  DO 500 I=1,921
    READ(13,5) WV,A3(I,1),A3(I,2),A3(I,3),A3(I,4),A3(I,5),
$           A3(I,6),A3(I,7),A3(I,8)
500 CONTINUE

C READ IN CARBON MONOXIDE LINE SPACING COEFFICIENTS

  READ(13,4)
  DO 600 I=1,921
    READ(13,5) WV,A3L(I,1),A3L(I,2),A3L(I,3),A3L(I,4),A3L(I,5),
$           A3L(I,6),A3L(I,7),A3L(I,8)
600 CONTINUE

C CLOSE THE DATA FILE
  CLOSE(UNIT = 13)

C RETURN TO THE CALLING ROUTINE AND END THE SUBROUTINE
  RETURN
  END
C-----

```

```

SUBROUTINE EXPRESS
C*****
C*****
C THIS ROUTINE ASKS QUESTIONS TO THE PROGRAM USER. IT IS USED TO
C GET PROGRAM PARAMETERS SUCH AS TEMPERATURE,PRESSURE,PATH LENGTH,
C NUMBER AND TYPE OF CONSTITUENTS, ETC...
C
C-----LIST OF VARIABLES IN EXPRESS-----
C----- (NOT MENTIONED PREVIOUSLY)-----
C FNAME..CHARACTER VARIABLE, NAME OF OUTPUT DATA FILE
C I..INTEGER VARIABLE USED TO DISTINGUISH USER PREFERENCE OF
C WAVENUMBER OR WAVELENGTH
C AMOL(I)..ARRAY OF MOLE FRACTIONS
C
C DIMENSION STATEMENTS AND COMMON BLOCKS
COMMON/ STUFF/ T,P,PP(20),WV,FNAM1
COMMON/ THICK/ DELX,DELU(15)
COMMON/ WAVE/ WV1,WV2,INT,NDIV
COMMON/ MOLES/ AMOL(20)

CHARACTER*20 FNAM1

C USER ENTERS WAVELENGTH OR WAVENUMBER PREFERENCE
WRITE(*,*)
WRITE(*,*) ' Enter [1] wavelength (micrometer)'
WRITE(*,*) ' [2] wave number (cm**-1) '
READ(*,*) I

C USER ENTERS WAVELENGTH RANGE OF INTEREST
IF(I .EQ. 1) THEN
WRITE(*,*)
WRITE(*,*) ' Please Enter the wavelength range ...'
WRITE(*,*) ' NOTE: No less than 2 microns'
WRITE(*,*) ' NOTE: No greater than 25 microns'
READ(*,*) WV11,WV22

C CONVERT WAVELENGTH TO WAVENUMBER BECAUSE TABLES ARE IN WAVENUMBERS
WRITE(*,*) 'CONVERTING WV1 AND WV2....'
WV1 = 10000./WV22
WV2 = 10000./WV11
WRITE(*,*) 'WV1....',WV1
WRITE(*,*) 'WV2....',WV2

C USERS ENTERS WAVENUMBER RANGE OF INTEREST
ELSE
WRITE(*,*)
WRITE(*,*) ' Please Enter then wavenumber range ....'
WRITE(*,*) ' NOTE: No less than 400, No greater than 500 !!'
WRITE(*,*) ' NOTE: Inherent resolution is 5 wavenumbers'
READ(*,*) WV1,WV2
ENDIF

C USER INPUTS THE TEMPERATURE
WRITE(*,*)
WRITE(*,*) ' Please input the Temperature [K]....'
READ(*,*) T

C USER INPUTS THE PRESSURE
WRITE(*,*)
WRITE(*,*) ' Please input the total pressure [ATM]....'
READ(*,*) P

C MESSAGE TO THE USER
WRITE(*,*)
WRITE(*,*) ' These Molecular Constituents are CURRENTLY available'

```

```

WRITE(*,*)' in any combination:'
WRITE(*,*)' [1] H2O Water Vapor'
WRITE(*,*)' [2] CO2 Carbon Dioxide'
WRITE(*,*)' [3] CO Carbon Monoxide'
WRITE(*,*)' [4] NO Nitrogen Oxide'
WRITE(*,*)' [5] CN '
WRITE(*,*)' [6] OH '
WRITE(*,*)' [7] HCl '
WRITE(*,*)' [8] HF '
WRITE(*,*)' [9] N2 Nitrogen'
WRITE(*,*)' [10] O2 Oxygen '
WRITE(*,*)' [11] H2 Hydrogen'

WRITE(*,*)
WRITE(*,*)' Only Constituents [1],[2],[3] will absorb or emit'
WRITE(*,*)' radiation. Constituents [4] through [11] will act'
WRITE(*,*)' to broaden the effects of [1],[2], and [3].'
```

C INITIALIZE VALUES OF THE MOLE FRACTIONS,PARTIAL PRESSURES

```

DO 56 I=1,20
  AMOL(I) = 0.
  PP(I) = 0.
56 CONTINUE
```

C USER INPUTS THE PARTICULAR CONSTITUENT AND MOLE FRACTIONS

```

WRITE(*,*)
WRITE(*,*)' Description of the Gas..... '
WRITE(*,*)
WRITE(*,*)' PLEASE Enter mole fraction of [1] H2O Water Vapor'
READ(*,*) AMOL(1)
WRITE(*,*)' PLEASE Enter mole fraction of [2] CO2 Carbon Dioxide'
READ(*,*) AMOL(2)
WRITE(*,*)' PLEASE Enter mole fraction of [3] CO Carbon Monoxide'
READ(*,*) AMOL(3)
WRITE(*,*)' PLEASE Enter mole fraction of [4] NO Nitrogen Oxide'
READ(*,*) AMOL(4)
WRITE(*,*)' PLEASE Enter mole fraction of [5] CN '
READ(*,*) AMOL(5)
WRITE(*,*)' PLEASE Enter mole fraction of [6] OH '
READ(*,*) AMOL(6)
WRITE(*,*)' PLEASE Enter mole fraction of [7] HCl '
READ(*,*) AMOL(7)
WRITE(*,*)' PLEASE Enter mole fraction of [8] HF '
READ(*,*) AMOL(8)
WRITE(*,*)' PLEASE Enter mole fraction of [9] N2 Nitrogen '
READ(*,*) AMOL(9)
WRITE(*,*)' PLEASE Enter mole fraction of [10] O2 Oxygen '
READ(*,*) AMOL(10)
WRITE(*,*)' PLEASE Enter mole fraction of [11] Hydrogen'
READ(*,*) AMOL(11)
```

C COMPUTE THE PARTIAL PRESSURES

```

DO 58 I=1,20
  PP(I) = P*AMOL(I)
58 CONTINUE
```

C ENTER THE PATH LENGTH

```

WRITE(*,*)
WRITE(*,*)' Please Enter the Path Length [CM].....'
READ(*,*) DELX
```

C ENTER THE OUTPUT DATA FILENAMES

```

WRITE(*,*)
```

```
        WRITE(*,*)' Please Enter the output data filename...'  
        READ(*,'(A20)') FNAM1  
C RETURN TO THE CALLING ROUTINE AND END THE SUBROUTINE  
  RETURN  
  END
```

C-----


```

SUBROUTINE SKATEPRO
C*****
C*****
C THIS ROUTINE TAKES THE ARRAYS CONTAINING THE ABSORPTION
C COEFFICIENTS AND LINE SPACING COEFFICIENTS FOR EACH SPECIES AND
C CREATES TWO NEW ARRAYS CONTAINING THOSE COEFFICIENTS SPECIFIC
C TO THE CURRENT TEMPERATURE.
C
C-----LIST OF VARIABLES IN SKATEPRO-----
C----- (NOT MENTIONED PREVIOUSLY) -----
C INT1..INTEGER VALUE USED TO ROUND OFF LOWER WAVENUMBER LIMIT
C INT2..INTEGER VALUE USED TO ROUND OFF UPPER WAVENUMBER LIMIT
C I1..LINE NUMBER BELOW WAVENUMBER OF INTEREST
C I2..LINE NUMBER ABOVE WAVENUMBER OF INTEREST
C J1..COLUMN NUMBER BELOW TEMPERATURE OF INTEREST
C J2..COLUMN NUMBER ABOVE TEMPERATURE OF INTEREST
C PERT..PERCENT USED TO LINEARLY INTERPOLATE BETWEEN TWO COLUMNS
C
C DIMENSION STATEMENTS AND COMMON BLOCKS
COMMON/ SPACE/ AKAP(12,999),SPAC(12,999)
COMMON/ NIRDATA/ A1(999,12),A1L(999,12),A2(999,12),
$      A2L(999,12),A3(999,12),A3L(999,12)
COMMON/ STUFF/ T,P,PP(20),WV,FNAM1
COMMON/ WAVE/ WV1,WV2,INT,NDIV
COMMON/ MOLES/ AMOL(20)

CHARACTER*20 FNAM1,FLIPPER

FLIPPER='ABSTEST.DAT'
OPEN(UNIT=7,FILE=FLIPPER,STATUS='UNKNOWN')

C ROUND OFF USER ENTERED VALUES FOR BEGINNING AND ENDDING WAVENUMBER
C SO THAT THOSE LIMITS ARE DIVISIBLE EXACTLY BY 5
INT1 = WV1/5
INT2 = WV2/5
WV1 = INT1 * 5.
WV2 = INT2 * 5.

C DETERMINE LINE NUMBER IN DATA FILE THAT CORRESPONDS TO THE LINE
C NUMBER OF THE BEGINNING WAVENUMBER (I1)
I1 = (WV1/5.) - 79

C DETERMINE THE NUMBER OF LINES IN DATA FILE BETWEEN THE BEGINNING
C WAVENUMBER AND THE ENDING WAVENUMBER
NDIV = (WV2 - WV1)/5. + 1

IF( T .LT. 100.) THEN
WRITE(*,*)' TEMPERATURE IS OUT OF RANGE AND IS SET'
WRITE(*,*)' EQUAL TO 100 K'
T = 100.
J1 = 1
PERT = 0.
ELSE IF ((T .GE. 100.) .AND. (T .LT. 200.)) THEN
J1 = 1
PERT = (T - 100.)/100.
ELSE IF ((T .GE. 200.) .AND. (T .LT. 300.)) THEN
J1 = 2
PERT = (T - 200.)/100.
ELSE IF ((T .GE. 300.) .AND. (T .LT. 600.)) THEN
J1 = 3
PERT = (T - 300.)/300.
ELSE IF ((T .GE. 600.) .AND. (T .LT. 1200.)) THEN
J1 = 4
PERT = (T - 600.)/600.
ELSE IF ((T .GE. 1200.) .AND. (T .LT. 1800.)) THEN

```

```

      J1 = 5
      PERT = (T - 1200.)/600.
      ELSE IF ((T .GE. 1800.) .AND. (T .LT. 2400.)) THEN
        J1 = 6
        PERT = (T - 1800.)/600.
      ELSE IF ((T .GE. 2400.) .AND. (T .LT. 3000.)) THEN
        J1 = 7
        PERT = (T - 2400.)/600.
      ELSE
        WRITE(*,*)' TEMPERATURE IS OUT OF RANGE AND IS SET'
        WRITE(*,*)' EQUAL TO 3000 K '
        T = 3000.
        PERT = 0.
      ENDIF

      J2 = J1 + 1

      WRITE(7,*)' BEGINNING WAVENUMBER....',WV1
      WRITE(7,*)' ENDING WAVENUMBER.....',WV2
      WRITE(7,*)' BEGINNING ROW, I1.....',I1
      WRITE(7,*)' NUMBER OF DIVISIONS.....',NDIV
      WRITE(7,*)' BEGINNING COLUMN, J1.....',J1
      WRITE(7,*)' ENDING COLUMN, J2.....',J2
      WRITE(7,*)' PERCENTAGE BETWEEN COL..',PERT

C LINEARLY INTERPOLATE WITHIN THE DATA FILES TO COMPUTE THE
C ABSORPTION COEFFICIENT AND LINE SPACING COEFFICIENT FOR A
C SINGLE TEMPERATURE FOR ALL WAVELENGTHS WITHIN A WAVELENGTH
C BAND FOR CONSTITUENTS [1],[2],AND [3]. NOTE: THIS DATA
C IS AVAILABLE ONLY FOR THESE THREE CONSTITUENTS

      DO 138 I=1,3
      IF(AMOL(I) .EQ. 0.) GOTO 138
      K1 = I1
      DO 138 J=1,NDIV
      IF( I .EQ. 1) THEN
        CALL LINEAR(A1(K1,J1),A1(K1,J2),PERT,AKAP(I,J))
        CALL LINEAR(A1L(K1,J1),A1L(K1,J2),PERT,SPAC(I,J))
      ELSE IF( I .EQ. 2) THEN
        CALL LINEAR(A2(K1,J1),A2(K1,J2),PERT,AKAP(I,J))
        CALL LINEAR(A2L(K1,J1),A2L(K1,J2),PERT,SPAC(I,J))
      ELSE IF( I .EQ. 3) THEN
        CALL LINEAR(A3(K1,J1),A3(K1,J2),PERT,AKAP(I,J))
        CALL LINEAR(A3L(K1,J1),A3L(K1,J2),PERT,SPAC(I,J))
      ENDIF

      K1 = K1 + 1
138 CONTINUE

C ELIMINATE EXTREME VALUES AND AVOID DIVISION BY ZERO ERRORS
      DO 176 I=1,3
      DO 176 J=1,NDIV
      IF(SPAC(I,J) .LE. 1.E-30) SPAC(I,J)=1.E-30
      IF(SPAC(I,J) .GE. 1.E30 ) SPAC(I,J)=1.E30
      IF(AKAP(I,J) .LE. 1.E-30) AKAP(I,J)=1.E-30
      IF(AKAP(I,J) .GE. 1.E30 ) AKAP(I,J)=1.E30
176 CONTINUE

C CHECK VALUES.....CO2,300K
      WRITE(7,*)' WVNUMBER   H2O ABS   CO2 ABS   CO ABS'
      WV = WV1
      DO 177 J=1,NDIV
      WRITE(7,*)WV,AKAP(1,J),AKAP(2,J),AKAP(3,J)
      WV = WV + 5
177 CONTINUE

```

```
CLOSE(UNIT=7)
C RETURN TO THE CALLING ROUTINE AND END THE SUBROUTINE
  RETURN
  END
C-----
```

```

      SUBROUTINE LINEAR(A1,A2,PERT,AKKAP)
C*****
C*****
C THIS ROUTINE LINEARLY INTERPOLATES BETWEEN TWO VALUES A1
C AND A2 AND STORES THE VALUE IN THE VARIABLE AKKAP
C
C-----LIST OF VARIABLES IN LINEAR-----
C----- (NOT MENTIONED PREVIOUSLY)-----
C A1..FIRST NUMBER USED IN INTERPOLATION
C A2..SECOND NUMBER USED IN INTERPOLATION
C PERT..PERCENT USED TO LINEARLY INTERPOLATE BETWEEN A1 AND A2
C APPLE..VALUE TO BE ADDED OR SUBTRACTED FROM A1
C AKKAP..FINAL VALUE, THE INTERPOLATED VALUE BETWEEN A1 AND A2
C
C COMPUTE THE ABSOLUTE VALUE OF THE DIFFERENCE BETWEEN A1 AND A2
      DIFF = ABS( ABS(A1) - ABS(A2) )

C COMPUTE THE VALUE TO BE ADDED OR SUBTRACTED FROM A1
      APPLE = DIFF * PERT

C DECIDE IF YOU SHOULD ADD OR SUBTRACT APPLE BASED ON SIGN OF A1
C AND COMPUTE INTERPOLATED VALUE BETWEEN A1 AND A2
      IF( A1 .LE. A2) THEN
          AKKAP = A1 + APPLE
      ELSE
          AKKAP = A1 - APPLE
      ENDIF

C RETURN TO THE CALLING ROUTINE AND END THE SUBROUTINE
      RETURN
      END
C-----

```

```

SUBROUTINE DELTAU
C*****
C*****
C THIS ROUTINE COMPUTES THE RESULTING PATH LENGTH INCREMENT
C ADJUSTED TO STP CONDITIONS
C
C-----LIST OF VARIABLES IN DELTAU-----
C----- (NOT MENTIONED PREVIOUSLY)-----
C ALL VARIABLES HAVE BEEN PREVIOUSLY DEFINED
C
C DIMENSION STATEMENTS AND COMMON BLOCKS
COMMON/ THICK/ DELX, DELU(15)
COMMON/ STUFF/ T, P, PP(20), WV, FNAME1

CHARACTER*20 FNAME1
C COMPUTE THE ADJUSTED PATH LENGTH INCREMENT
DO 139 I=1,15
  DELU(I) = DELX * (273.15/T) * ( PP(I) / 1. )

139 CONTINUE
C RETURN TO THE CALLING ROUTINE AND END THE SUBROUTINE
RETURN
END
C-----

```

```

SUBROUTINE BROADEN
C*****
C*****
C THIS ROUTINE COMPUTES THE COLLISION BROADENED HALF WIDTH AND
C DOPPLER BROADENED HALF WIDTHS FOR ALL WAVELENGTHS OVER THE
C DESIGNATED WAVELENGTH INTERVAL
C
C-----LIST OF ARRAYS IN BROADEN-----
C----- (NOT MENTIONED PREVIOUSLY)-----
C GAMFB(12,12)..FOREIGN BROADENED COLLISION LINE WIDTH PARAMETER
C ETAFB(12,12)..FOREIGN BROADENED COLLISION LINE WIDTH PARAMETER
C GAMRB(12)..RESONANT BROADENED COLLISION LINE WIDTH PARAMETER
C ETARB(12,12)..RESONANT BROADENED COLLISION LINE WIDTH PARAMETER
C WTMOL(12)..ARRAY CONTAINING THE MOLECULAR WEIGHTS OF THE SPECIES
C
C DIMENSION STATEMENTS AND COMMON BLOCKS
COMMON/ STUFF/ T, P, PP(20), WV, FNAME1
COMMON/ GAMMA/ GAMC(20), GAMD(12,999)
COMMON/ DATA1/ GAMFB(12,12), ETAFB(12,12), GAMRB(12), ETARB(12,12)
COMMON/ DATA2/ WTMOL(12)
COMMON/ MOLES/ AMOL(20)

CHARACTER*20 FNAME1

C ROUTINE TO COMPUTE THE DOPPLER BROADENED HALF WIDTH
CALL DOPPHWD

C ROUTINE TO COMPUTE THE COLLISION BROADENED HALF WIDTH
CALL COLLHWD

C RETURN TO THE CALLING ROUTINE AND END THE SUBROUTINE
RETURN
END
C-----

```

```

SUBROUTINE DOPPHWD
C*****
C*****
C THIS ROUTINE COMPUTES THE DOPPLER BROADENED HALF WIDTH AT ALL
C WAVELENGTHS WITHIN THE WAVELENGTH INTERVAL, FOR EACH MOLECULAR
C SPECIES
C
C-----LIST OF VARIABLES IN DOPPHWD-----
C----- (NOT MENTIONED PREVIOUSLY)-----
C I..INTEGER VARIABLE USED TO INDEX THE CONSTITUENT
C J..INTEGER VARIABLE USED TO INDEX THE WAVENUMBER
C
C DIMENSION STATEMENTS AND COMMON BLOCKS
COMMON/ STUFF/ T,P,PP(20),WV,FNAM1
COMMON/ GAMMA/ GAMC(20),GAMD(12,999)
COMMON/ WAVE/ WV1,WV2,INT,NDIV
COMMON/ DATA2/ WTMOL(12)
CHARACTER*20 FNAM1

C GET THE MOLECULAR WEIGHTS OF THE GASEOUS CONSTITUENTS
CALL GETDAT2

C INDEX THE STARTING WAVENUMBER
WV = WV1

C COMPUTE THE DOPPLER BROADENED HALF WIDTH FOR EACH CONSTITUENT
C THIS EQUATION COMES FROM EQUATION 5-35 OF NASA SP-3080
DO 78 I=1,11

C RESET THE STARTING WAVENUMBER
WV = WV1

C INDEX OVER THE RANGE OF WAVENUMBERS
DO 78 J=1,NDIV
GAMD(I,J) = (5.94E-6)*WV/((WTMOL(I))**(0.5))*
$          ((T/273.15)**(0.5))

C INDEX THE WAVENUMBER AND CONTINUE WITH THE DO LOOP
WV = WV + 5.
78 CONTINUE

C RETURN TO THE CALLING ROUTINE AND END THE SUBROUTINE
RETURN
END
C-----

```

```

SUBROUTINE GETDAT2
C*****
C*****
C THIS ROUTINE READS IN THE MOLECULAR WEIGHTS OF THE GASEOUS
C CONSTITUENTS FROM A DATA FILE AND STORES THOSE VALUES IN
C AN ARRAY
C
C-----LIST OF VARIABLES IN GETDAT2-----
C----- (NOT MENTIONED PREVIOUSLY)-----
C FNAME..CHARACTER VARIABLE, NAME OF FILE CONTAINING
C      MOLECULAR WEIGHTS
C I..INTEGER VARIABLE, USED TO INDEX THE CONSTITUENT
C
C COMMON BLOCKS AND DIMENSION STATEMENTS
      CHARACTER*20 FNAME
      COMMON/ DATA2/ WTMOL(12)

C ESTABLISH THE NAME AND OPEN THE DATA FILE
      FNAME = 'MOLEWT.DAT'
      OPEN(UNIT=7, FILE= FNAME, STATUS = 'UNKNOWN' )

C SKIP THE FILE HEADER
      READ(7,1003)
1003 FORMAT(////)

C READ IN THE MOLECULAR WEIGHTS FROM A DATA FILE
      DO 92 I=1,11
        92 READ(7,*) WTMOL(I)

C CLOSE THE DATA FILE
      CLOSE(UNIT=7)

C RETURN TO THE CALLING ROUTINE AND END THE SUBROUTINE
      RETURN
      END
C-----

```



```

SUBROUTINE COLLHWD
C*****
C*****
C THIS ROUTINE COMPUTES THE COLLISION BROADENED HALF WIDTH AT ALL
C WAVELENGTHS WITHIN THE WAVELENGTH INTERVAL, FOR EACH MOLECULAR
C SPECIES
C
C-----LIST OF VARIABLES IN COLLHWD-----
C----- (NOT MENTIONED PREVIOUSLY)-----
C I..INTEGER VARIABLE, USED TO INDEX THROUGH EACH CONSTITUENT
C J..INTEGER VARIABLE, USED TO INDEX THROUGH EACH CONSTITUENT THAT
C   ACTS TO BROADEN THE EMISSION BY FOREIGN BROADENING
C GAMCA..INTERMEDIATE VALUE EQUIVALENT TO THE FOREIGN BROADENING
C   CONTRIBUTION OF THE COLLISION BROADENED HALF WIDTH
C GAMCB..INTERMEDIATE VALUE EQUIVALENT TO THE RESONANT BROADENING
C   CONTRIBUTION OF THE COLLISION BROADENED HALF WIDTH
C
C DIMENSION STATEMENTS AND COMMON BLOCKS
COMMON/ DATA1/ GAMFB(12,12),ETAFB(12,12),GAMRB(12),ETARB(12,12)
COMMON/ STUFF/ T,P,PP(20),WV,FNAM1
COMMON/ GAMMA/ GAMC(20),GAMD(12,999)
COMMON/ WAVE/ WV1,WV2,INT,NDIV

CHARACTER*20 FNAME1

C GET DATA FOR RESONANT AND COLLISION BROADENED HALF WIDTH
CALL GETDAT1

C COMPUTE THE COLLISION HALF WIDTH FOR THE Ith SPECIES
C THIS IS EQUATION 5-34 FROM NASA SP-3080
DO 73 I=1,8

C COMPUTE RESONANT BROADENING CONTRIBUTION OF THE COLLISION
C BROADENED HALF WIDTH
GAMCB = 0.0
GAMCB = GAMRB(I) * PP(I) * ((273./T)**
$ (ETARB(I,I) ) )

C COMPUTE FOREIGN BROADENING CONTRIBUTION OF THE COLLISION
C BROADENED HALF WIDTH
GAMCA = 0.
DO 71 J=1,11
GAMCA = GAMCA + GAMFB(I,J)*PP(J)*((273./T)**
$ (ETAFB(I,J) ) )
71 CONTINUE

C STORE THAT VALUE IN AN ARRAY AND CONTINUE WITH THE DO LOOP
GAMC(I) = GAMCA + GAMCB
73 CONTINUE

C RETURN TO THE CALLING ROUTINE AND END THE SUBROUTINE
RETURN
END
C-----

```

```

SUBROUTINE GETDAT1
C*****
C*****
C THIS ROUTINE READS IN THE VALUES FOR THE RESONANT AND COLLISION
C BROADENED HALF WIDTH FROM A FILE AND STORES THOSE VALUES IN
C ARRAYS.  THESE VALUES ARE LISTED IN TABLE 5-19 OF NASA SP-3080.
C
C-----LIST OF VARIABLES IN GETDAT1-----
C----- (NOT MENTIONED PREVIOUSLY)-----
C FNAM..CHARACTER VARIABLE, NAME OF DATA FILE CONTAINING COLLISION
C     LINE WIDTH PARAMETERS
C
C DIMENSION STATEMENTS AND COMMON BLOCKS
      CHARACTER*20 FNAM
      COMMON/ DATA1/ GAMFB(12,12), ETAFB(12,12), GAMRB(12), ETARB(12,12)

C ESTABLISH DATA FILE NAME
      FNAM = 'COLLIDE.DAT'

C OPEN DATA FILE CONTAINING MODEL VALUES FOR THE COLLISION LINE WIDTH
C PARAMETERS, AND READ PAST HEADER FOR THAT FILE
      OPEN(UNIT = 6, FILE = FNAM, STATUS = 'UNKNOWN')
      READ(6,1006)
      1006 FORMAT(////)

C READ DATA FROM DATA FILE, ARRAY FOR THE FOREIGN BROADENED COLLISION
C LINE WIDTH PARAM GAMMA
      DO 86 I=1,11
        86 READ(6,*) GAMFB(I,1),GAMFB(I,2),GAMFB(I,3),GAMFB(I,4),GAMFB(I,5),
          $          GAMFB(I,6),GAMFB(I,7),GAMFB(I,8),GAMFB(I,9),GAMFB(I,10),
          $          GAMFB(I,11)

C READ DATA FROM DATA FILE, ARRAY FOR THE RESONANT BROADENED COLLISION
C LINE WIDTH PARAM GAMMA
      READ(6,1007)
      1007 FORMAT(///)
      READ(6,*) GAMRB(1),GAMRB(2),GAMRB(3),GAMRB(4),GAMRB(5),
        $      GAMRB(6),GAMRB(7),GAMRB(8)

C CLOSE THE DATA FILE
      CLOSE(UNIT = 6)

C FILL IN ARRAY FOR RESONANT BROADENED COLLISION LINE WIDTH PARAM ETA
      DO 87 I=1,11
        87 ETARB(I,I) = 1.0

C FILL IN ARRAY FOR FOREIGN BROADENED COLLISION LINE WIDTH PARAM ETA
      DO 97 J=1,11
      DO 97 I=1,11
        97 ETAFB(I,J) = 0.5

C RETURN TO CALLING ROUTINE AND END THE SUBROUTINE
      RETURN
      END
C-----

```

```

SUBROUTINE STAR
C*****
C*****
C ROUTINE TO COMPUTE THE OPTICAL DEPTH FOR THE WEAK LINE LIMIT
C
C-----LIST OF VARIABLES IN STAR-----
C----- (NOT MENTIONED PREVIOUSLY)-----
C I..INTEGER VARIABLE USED TO INDEX THROUGH THE CONSTITUENTS
C J..INTEGER VARIABLE USED TO INDEX THROUGH THE WAVENUMBERS
C JJ..INTEGER VARIABLE IDENTIFYING THE PARTICULAR CONSTITUENT
C
C DIMENSION STATEMENTS AND COMMON BLOCKS
COMMON/ STUFF/ T,P,PP(20),WV,FNAM1
COMMON/ THICK/ DELX,DELU(15)
COMMON/ SPACE/ AKAP(12,999),SPAC(12,999)
COMMON/ STARDM/ XSTAR(12,999)
COMMON/ WAVE/ WV1,WV2,INT,NDIV
COMMON/ MOLES/ AMOL(20)

CHARACTER*20 FNAM1

C COMPUTE THE OPTICAL DEPTH FOR THE WEAK LINE LIMIT FOR EVERY
C WAVENUMBER IN THE WAVENUMBER RANGE FOR GASEOUS CONSTITUENTS
C [1],[2],OR [3]
DO 103 I = 1,3
IF (AMOL(I) .EQ. 0.) THEN
GOTO 103
ENDIF

DO 103 J=1,NDIV

C THIS EQUATION FOLLOWS FROM EQUATION 5-27 OF NASA SP-3080
XSTAR(I,J) = AKAP(I,J) * DELU(I)
IF(XSTAR(I,J) .LE. 1.E-11) XSTAR(I,J)=1.E-11
IF(XSTAR(I,J) .GE. 1.E11) XSTAR(I,J)=1.E11
103 CONTINUE

C RETURN TO THE CALLING ROUTINE AND END THE SUBROUTINE
RETURN
END
C-----

```

```

SUBROUTINE FINER
C*****
C*****
C ROUTINE TO COMPUTE THE COLLISION AND DOPPLER BROADENED FINE
C STRUCTURE PARAMETER AT ALL WAVENUMBERS WITHIN THE WAVENUMBER RANGE
C FOR EACH GASEOUS CONSTITUENT
C
C-----LIST OF VARIABLES IN FINER-----
C----- (NOT MENTIONED PREVIOUSLY)-----
C DOPP..INTERMEDIATE VARIABLE USED TO COMPUTE THE DOPPLER
C      BROADENED FINE STRUCTURE PARAMETER
C COLL..INTERMEDIATE VARIABLE USED TO COMPUTE THE
C      COLLISION BROADENED FINE STRUCTURE PARAMETER
C I..INTEGER VARIABLE, USED TO IDENTIFY SPECIES
C II..INTEGER VARIABLE, USED TO INDEX THROUGH THE SPECIES
C J..INTEGER VARIABLE, USED TO INDEX THROUGH THE WAVENUMBERS
C
C DIMENSION STATEMENTS AND COMMON BLOCKS
COMMON/ STUFF/ T, P, PP(20), WV, FNAME1
COMMON/ WAVE/ WV1, WV2, INT, NDIV
COMMON/ THICK/ DELX, DELU(15)
COMMON/ STARDM/ XSTAR(12,999)
COMMON/ SPACE/ AKAP(12,999), SPAC(12,999)
COMMON/ GAMMA/ GAMC(20), GAMD(12,999)
COMMON/ FINEST/ ASUBD(12,999), ASUBC(12,999)
COMMON/ MOLES/ AMOL(20)

CHARACTER*20 FNAME1

C COMPUTE THE COLLISION AND DOPPLER BROADENED FINE STRUCTURE
C PARAMETERS, FROM EQUATION 5-30 AND 5-31, NASA SP-3080

C INDEX THROUGH EMITTING CONSTITUENTS
DO 104 I=1,3

C CHECK PRESENTS OF CONSTITUENTS
IF(AMOL(I) .EQ. 0.) GOTO 104

C INDEX THROUGH WAVENUMBERS
DO 104 J=1,NDIV

C COMPUTE DOPPLER BROADENED FINE STRUCTURE PARAMETER
ASUBD(I,J) = GAMD(I,J)*SPAC(I,J)

C COMPUTE COLLISION BROADENED FINE STRUCTURE PARAMETER
ASUBC(I,J) = GAMC(I) * SPAC(I,J)

C AVOID DIVISION BY ZERO ERROR
IF(ASUBD(I,J) .LE. 1.E-22) ASUBD(I,J)=1.E-22
IF(ASUBD(I,J) .GE. 1.E22) ASUBD(I,J)=1.E22
IF(ASUBC(I,J) .LE. 1.E-22) ASUBC(I,J)=1.E-22
IF(ASUBC(I,J) .GE. 1.E22) ASUBC(I,J)=1.E22
104 CONTINUE

C RETURN TO THE CALLING ROUTINE AND END THE SUBROUTINE
RETURN
END
C-----

```

```

SUBROUTINE GROWTH
C*****
C*****
C COMPUTE THE OPTICAL DEPTH FOR A PURE DOPPLER CURVE OF GROWTH AND
C A PURE COLLISION CURVE OF GROWTH
C
C-----LIST OF VARIABLES IN GROWTH-----
C----- (NOT MENTIONED PREVIOUSLY) -----

C DIMENSION STATEMENTS AND COMMON BLOCKS
COMMON/ STUFF/ T,P,PP(20),WV,FNAM1
COMMON/ WAVE/ WV1,WV2,INT,NDIV
COMMON/ STARDM/ XSTAR(12,999)
COMMON/ FINEST/ ASUBD(12,999),ASUBC(12,999)
COMMON/ DEPTH/ XSUBD(12,999),XSUBC(12,999)
COMMON/ MOLES/ AMOL(20)

CHARACTER*20 FNAM1

C INDEX THROUGH CONSTITUENTS
DO 106 I=1,3

C CHECK PRESENTS OF CONSTITUENTS
IF(AMOL(I) .EQ. 0.) GOTO 106

C INDEX THROUGH THE WAVENUMBERS
DO 106 J=1,NDIV

C INTERMEDIATE VALUE
ARG = 1. + ( XSTAR(I,J)/1.7/ASUBD(I,J) )**2.

C COMPUTE THE OPTICAL DEPTH FOR A PURE DOPPLER CURVE OF GROWTH
C FROM EQUATION 5-29, NASA SP-3080

IF(ARG .LE. 1.000001) THEN
C AVOID DIVISION BY ZERO ERROR
XSUBD(I,J) = 0.0
ELSE
XSUBD(I,J) = 1.7*ASUBD(I,J)*SQRT( LOG( ARG ) )
ENDIF

C AVOID DIVISION BY ZERO ERROR
IF(XSUBD(I,J) .LE. 1.E-11) XSUBD(I,J)=1.E-11
IF(XSUBD(I,J) .GE. 1.E11 ) XSUBD(I,J)=1.E11

C COMPUTE THE OPTICAL DEPTH FOR A PURE COLLISION CURVE OF GROWTH
C FROM EQUATION 5-28, NASA SP-3080
XSUBC(I,J)= XSTAR(I,J)/SQRT(1.+XSTAR(I,J)/4./ASUBC(I,J))

C AVOID DIVISION BY ZERO ERROR
IF(XSUBC(I,J) .LE. 1.E-11) XSUBC(I,J)=1.E-11
IF(XSUBC(I,J) .GE. 1.E11 ) XSUBC(I,J)=1.E11
106 CONTINUE

C RETURN TO THE CALLING ROUTINE AND END THE SUBROUTINE
RETURN
END
C-----

```

```

SUBROUTINE OPCLOD
C*****
C*****
C THIS ROUTINE COMPUTES THE COMBINED COLLISION AND DOPPLER OPTICAL
C DEPTHS
C
C-----LIST OF VARIABLES IN OPCLOD-----
C----- (NOT MENTIONED PREVIOUSLY)-----

C DIMENSION STATEMENTS AND COMMON BLOCKS
CHARACTER*20 FNAME1
CHARACTER*50 AOPTION
COMMON/ STUFF/ T, P, PP(20), WV, FNAME1
COMMON/ WAVE/ WV1, WV2, INT, NDIW
COMMON/ DEPTH/ XSUBD(12,999), XSUBC(12,999)
COMMON/ STARDM/ XSTAR(12,999)
COMMON/ OPTIC/ YSUBN(12,999), XSUBN(12,999), X(999)
COMMON/ THICK/ DELX, DELU(15)
COMMON/ MOLES/ AMOL(20)
COMMON/ RESULT/ ABS(999), TRANS(999)

C INDEX THROUGH EMMITING CONSTITUENTS
DO 107 I=1,3

C CHECK PRESENCE OF CONSTITUENTS
IF(AMOL(I) .EQ. 0.) GOTO 107

C REINITIALIZE BEGINNING WAVENUMBER
WV = WV1

C INDEX THROUGH WAVENUMBERS
DO 107 J=1,NDIV
WRITE(8,*) 'WAVENUMBER...', WV

C COMPUTE OPTICAL DEPTH FOR INDIVIDUAL SPECIES IN THE
C VOLUME ELEMENT

C INTERMEDIATE VALUES
XCXS = XSUBC(I,J)/XSTAR(I,J)
XDXS = XSUBD(I,J)/XSTAR(I,J)

C AVOID DIVISION BY ZERO ERROR
IF(XCXS .EQ. 1.0) XCXS=0.9999999
IF(XDXS .EQ. 1.0) XDXS=0.9999999

C INTERMEDIATE VALUES
ARG1 = (1./ ( 1. - (XCXS)**2. ))**2.
ARG2 = (1./ ( 1. - (XDXS)**2. ))**2.

C AVOID DIVISION BY ZERO ERROR
IF(ARG1 .LE. 1.E-30) ARG1=1.E-30
IF(ARG1 .GE. 1.E30 ) ARG1=1.E30
IF(ARG2 .LE. 1.E-30) ARG2=1.E-30
IF(ARG2 .GE. 1.E30 ) ARG2=1.E30

C COMPUTE THE COMBINED COLLISION AND DOPPLER OPTICAL DEPTHS
YSUBN(I,J) = ARG1 + ARG2 - 1.

C COMPUTE THE OPTICAL DEPTH FOR THE PARTICULAR CONSTITUENT
XSUBN(I,J) = (SQRT( 1.- (1./SQRT(YSUBN(I,J)))))*XSTAR(I,J)

C INDEX THE WAVENUMBER
WV = WV + 5
107 CONTINUE

```

```

C COMPUTE OPTICAL DEPTH FOR THE GASEOUS MIXTURE AS A FUNCTION
C OF WAVENUMBER

C INITIALIZE OPTICAL DEPTH AS ZERO
  XX = 0.

C INDEX THROUGH WAVENUMBERS
  DO 109 J=1,NDIV

C INDEX THROUGH EMITTING CONSTITUENTS
  DO 108 I=1,3

C CHECK FOR PRESENTS OF CONSTITUENTS
  IF (AMOL(I) .EQ. 0.) GOTO 108

C SUM OPTICAL DEPTHS FROM ALL CONSTITUENTS
  XX = XX + XSUBN(I,J)
108 CONTINUE

C STORE MIXTURE OPTICAL DEPTH IN AN ARRAY
  X(J) = XX

C COMPUTE ABSORPTIVITY FROM THE OPTICAL DEPTH AND
C STORE THAT VALUE IN AN ARRAY
  ABS(J) = 1.-EXP(-XX)

C COMPUTE THE TRANSMITTANCE
  TRANS(J) = EXP(-XX)

C RESET OPTICAL DEPTH TO ZERO FOR A NEW WAVENUMBER
  XX = 0
109 CONTINUE

C RETURN TO THE CALLING ROUTINE AND END THE SUBROUTINE
  RETURN
  END
C-----

```

```

SUBROUTINE WRITER
C*****
C*****
C THIS ROUTINE WRITES DATA TO A FILE
C
C-----LIST OF VARIABLES IN WRITER-----
C----- (NOT MENTIONED PREVIOUSLY) -----

C DIMENSION STATEMENTS AND COMMON BLOCKS

COMMON/ STUFF/ T,P,PP(20),WV,FNAM1
COMMON/ WAVE/ WV1,WV2,INT,NDIV
COMMON/ DEPTH/ XSUBD(12,999),XSUBC(12,999)
COMMON/ STARDM/ XSTAR(12,999)
COMMON/ OPTIC/ YSUBN(12,999),XSUBN(12,999),X(999)
COMMON/ THICK/ DELX,DELU(15)
COMMON/ MOLES/ AMOL(20)
COMMON/ RESULT/ ABS(999),TRANS(999)

CHARACTER FNAM1*20,AOPTION*50,AHEAD*5

C OPEN OUTPUT DATA FILE
OPEN(UNIT = 0,FILE = FNAM1,STATUS = 'UNKNOWN')

C USER TURN ON/OFF OUTPUT FILE HEADER
WRITE(*,*)
WRITE(*,*) ' Do you want a file header ? [y/n]'
READ(*,'(A5)') AHEAD
IF( (AHEAD.EQ. 'N') .OR. (AHEAD.EQ. 'n') ) THEN
  GOTO 1049
ENDIF

C WRITE FILE HEADER TO DATA FILE
WRITE(0,1010)T,P,DELX,WV1,WV2
1010 FORMAT(2X,'PROGRAM SAIL OUTPUT',/,/,
$      2X,'TEMPERATURE           = ',F10.2,/,
$      2X,'TOTAL PRESSURE        = ',F10.2,/,
$      2X,'PATH LENGTH (cm)      = ',F10.2,/,
$      2X,'STARTING WAVENUMBER   = ',F10.2,/,
$      2X,'ENDING WAVENUMBER    = ',F10.2,/)

WRITE(0,1017)
1017 FORMAT(2X,'MOLE FRACTIONS OF CONSTITUENTS:',/,/)

C WRITE MOLE FRACTION TO DATA FILE
WRITE(0,1018) AMOL(1),AMOL(2),AMOL(3),AMOL(4),AMOL(5),
$            AMOL(6),AMOL(7),AMOL(8),AMOL(9),AMOL(10),
$            AMOL(11)
1018 FORMAT(2X,'H2O ..',F10.6,3X,'CO2...',F10.6,/,
$      2X,'CO....',F10.6,3X,'NO....',F10.6,/,
$      2X,'CN....',F10.6,3X,'OH....',F10.6,/,
$      2X,'HCl...',F10.6,3X,'HF....',F10.6,/,
$      2X,'N2....',F10.6,3X,'O2....',F10.6,/,
$      2X,'H2....',F10.6)

C WRITE COLUMN HEADER
WRITE(0,1019)
1019 FORMAT(/,2X,'WAVENUMBER',5X,'ABSORPTIVITY',3X,
$          'TRANSMITTANCE',/)

C WRITE DATA TO A FILE
1049 CONTINUE

C REINITIALIZE BEGINNING WAVENUMBER
WV = WV1

```



```
C INDEX THROUGH WAVENUMBERS
  DO 167 J=1,NDIV

C WRITE THIS DATA TO A FILE
  WRITE(0,*) WV,ABS(J),TRANS(J)

C INDEX WAVENUMBER
  WV = WV + 5
167 CONTINUE

C CLOSE THE DATA FILE
  CLOSE(UNIT = 0)

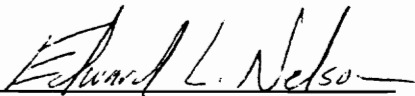
C RETURN TO CALLING ROUTINE AND END THE SUBROUTINE
  RETURN
  END
```

Vita

Edward L. Nelson is a native of Christiansburg, VA. He graduated from Christiansburg High School in June 1986. In 1986 he received a full tuition, four year scholarship from the National Society of Professional Engineers to attend Virginia Polytechnic Institute and State University, Virginia Tech. Edward graduated from Virginia Tech with a Bachelor of Science in Mechanical Engineering in May 1990. While at Virginia Tech, he was inducted into the Mortar Board National Honor Society and became a life member of Alpha Phi Omega National Service Fraternity. During the summers, Edward worked for Hercules Powder Company, Radford, VA, and Lord Corporation, Erie, PA.

In May 1990, Edward started his graduate studies at Virginia Tech. He worked as a graduate cooperative education student at the National Aeronautics and Space Administration (NASA) at Ames Research Center in Moffett Field, CA.

Nelson hopes pursue a Doctor of Philosophy in Mechanical Engineering from Virginia Tech under the direction of J.R. Mahan and with funding from the NASA Ames Postbaccalaureate Program.


Edward L. Nelson